

THE DWARF SPHEROIDAL COMPANIONS TO M31: VARIABLE STARS IN ANDROMEDA I AND ANDROMEDA III¹

BARTON J. PRITZL² AND TAFT E. ARMANDROFF

National Optical Astronomy Observatory, P.O. Box 26732, Tucson, AZ 85726
 email: pritzl@noao.edu, armand@noao.edu

GEORGE H. JACOBY

WIYN Observatory, P.O. Box 26732, Tucson, AZ, 85726
 email: gjacoby@wiyn.org

G. S. DA COSTA

Research School of Astronomy and Astrophysics, Institute of Advanced Studies, The Australian National University, Cotter Road, Weston, ACT 2611,
 Australia
 email: gdc@mso.anu.edu.au

AJ, in press

ABSTRACT

We present the results of variable star searches of the M31 dwarf spheroidal companions Andromeda I and Andromeda III using the *Hubble Space Telescope*. A total of 100 variable stars were found in Andromeda I, while 56 were found in Andromeda III. One variable found in Andromeda I and another in Andromeda III may be Population II Cepheids. In addition to this variable in Andromeda III, another four variables are anomalous Cepheids. So far, no definite anomalous Cepheids have been discovered in Andromeda I. We discuss the properties of these variables with respect to those found in the other dwarf spheroidal galaxies and revisit the anomalous Cepheid period-luminosity relations. We found 72 fundamental mode RR Lyrae stars and 26 first-overtone mode RR Lyrae stars in Andromeda I giving mean periods of 0.575 day and 0.388 day, respectively. One likely RR Lyrae in Andromeda I remains unclassified due to a lack of F555W data. For Andromeda III, 39 RR Lyrae stars are pulsating in the fundamental mode with a mean period of 0.657 day and 12 are in the first-overtone mode with a mean period of 0.402 day. Using the mean metal abundances derived from the red giant branch colors, the mean RRab period for Andromeda I is consistent with the mean period - metallicity relation seen in the RR Lyrae populations of Galactic globular clusters, while Andromeda III is not, having too large a mean RRab period for its abundance. In Andromeda I, we found two RR Lyrae stars which are noticeably fainter than the horizontal branch. We discuss the possibility that these stars are associated with the recently discovered stellar stream in the halo of M31.

Using various methods, we estimate the mean metallicity of the RR Lyrae stars to be $\langle \text{[Fe/H]} \rangle \approx -1.5$ for Andromeda I and ≈ -1.8 for Andromeda III. These estimates match well with other mean metallicity estimates for the galaxies. Interestingly, a comparison of the period-amplitude diagrams for these two galaxies with other dwarf spheroidal galaxies shows that Andromeda III is lacking in shorter period, higher amplitude RR Lyrae stars. This may be a consequence of the very red horizontal branch morphology in this dSph. Not including the two faint RR Lyrae stars, we find $\langle V_{\text{RR}} \rangle = 25.14 \pm 0.04$ mag for Andromeda I resulting in a distance of 765 ± 25 kpc. For Andromeda III, $\langle V_{\text{RR}} \rangle = 25.01 \pm 0.04$ mag giving a distance of 740 ± 20 kpc. These distance estimates are consistent with those previously found for these galaxies. We discuss the relation between the specific frequency of the anomalous Cepheids in dwarf spheroidal galaxies and the mean metallicity of the galaxy, finding that the M31 dwarf spheroidal galaxies follow the same relations as the Galactic dwarf spheroidal galaxies. We also find that the period-luminosity relations of anomalous Cepheids and short-period Cepheids are distinct, with the short-period Cepheids having higher luminosities at a given period.

Subject headings: Cepheids — galaxies: individual (Andromeda I; Andromeda III) — Local Group — RR Lyrae variables — stars: variables: other

1. INTRODUCTION

The Galactic dwarf spheroidal (dSph) galaxies are known to have a diversity of star formation histories, from mainly old (age > 10 Gyr) stellar populations such as Ursa Minor (e.g., Olszewski & Aaronson 1985), to Fornax which had star for-

mation as late as 0.3-0.4 Gyrs ago (Saviane, Held, & Bertelli 2000). While there have been many studies of the Galactic dSph galaxies, until recently little was known about the stellar populations of the M31 dSph galaxies. In fact, it was only in the past few years that half of the known M31 dSph galaxies were discovered (Andromeda V: Armandroff, Davies, & Jacoby 1998; Andromeda VI [Pegasus]: Armandroff, Jacoby, & Davies 1999, Karachentsev & Karachentseva 1999; Andromeda VII [Cassiopeia]: Karachentsev & Karachentseva 1999).

A series of observations of the M31 dSph galaxies with the

¹ Based on observations with the NASA/ESA *Hubble Space Telescope*, obtained at the Space Telescope Science Institute, which is operated by the Association of Universities for Research in Astronomy, Inc., (AURA), under NASA Contract NAS 5-26555.

² Current address: Department of Physics and Astronomy, Macalester College, 1600 Grand Ave., Saint Paul, MN 55105; pritzl@macalester.edu

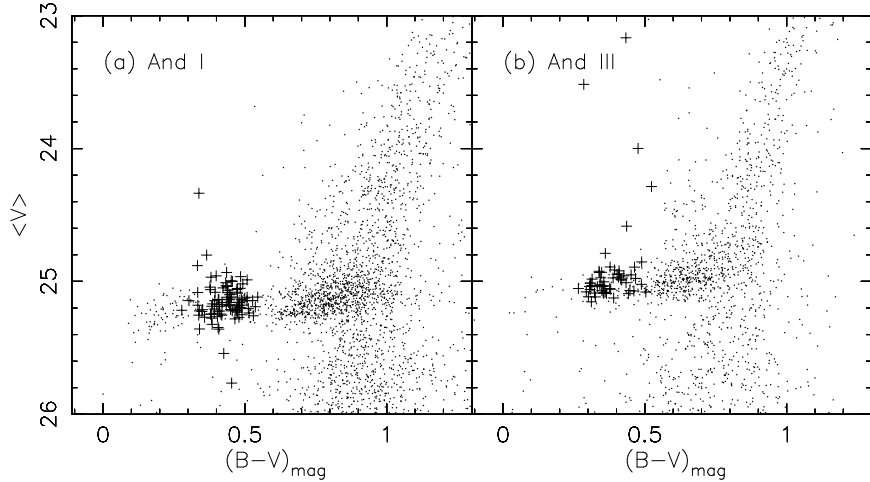


FIG. 1.— And I (a) and And III (b) color-magnitude diagrams using the photometry of DACS00 and DAC02 except for the variable stars identified in this work which are plotted as plus signs. The anomalous Cepheids or Population II Cepheids occur above the level of the horizontal branch. In addition, we note the presence of two fainter RR Lyrae in the And I color-magnitude diagram.

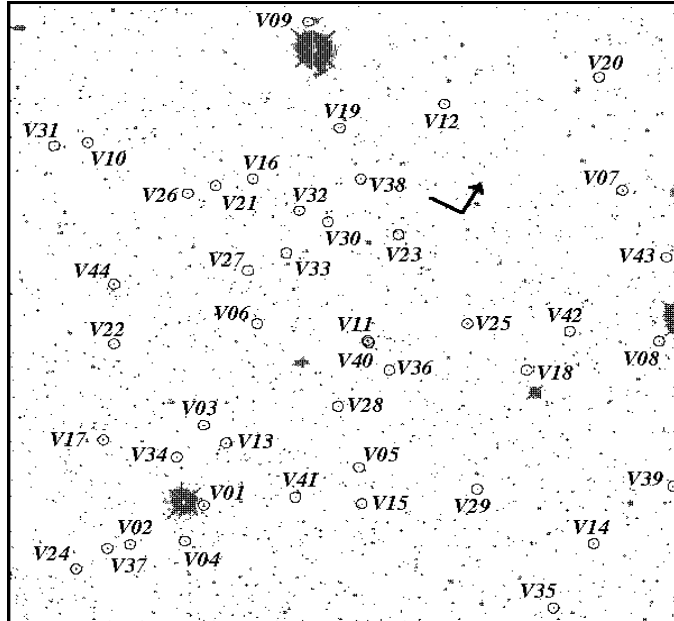


FIG. 2.— Finding charts for the And I variable stars. The WFC2 ($1.2' \times 1.3'$), WFC3 ($1.3' \times 1.2'$), and WFC4 ($1.2' \times 1.2'$) images are each shown in a panel. North and east directions are shown with the arrow pointing toward the north.

Hubble Space Telescope (HST) Wide Field Planetary Camera 2 (WFPC2) has been used to investigate their stellar populations to levels fainter than the horizontal branch (HB). We are also able to use these observations to investigate the variable star content of these dSph galaxies. The variable star content is important because it provides insight to the age, metallicity, and distance to the galaxy in which the variables are found. We have already discussed the variable stars in Andromeda VI (And VI; Pritzl et al. 2002; henceforth Paper I) and Andromeda II (And II; Pritzl et al. 2004; henceforth Paper II). In this third paper of the series, we investigate the variable stars in Andromeda I (And I) and Andromeda III (And III).

Of the M31 dSph companions, And I lies closest to M31. It is also on the high end of the metallicities for dSph galaxies ($\langle \text{[Fe/H]} \rangle = -1.46 \pm 0.12$; Da Costa et al. 2000, henceforth

DACS00). The color-magnitude diagram (CMD) shows the typical properties seen in other dSph galaxies such as a predominantly red HB and an internal abundance spread. A radial gradient in the HB stars was also detected where there are relatively more blue HB stars beyond the core radius of the galaxy (Da Costa et al. 1996; henceforth DACS96).

And III also lies in the outer halo of M31 and is the next closest dSph to M31 after And I. The HB in the CMD for this dSph galaxy is significantly redder than that seen in the other M31 dSph galaxies that have been observed. And III is also one of the most metal-poor of the M31 dSph companions ($\langle \text{[Fe/H]} \rangle = -1.88 \pm 0.11$; Da Costa, Armandroff, & Caldwell 2002, henceforth DAC02). Further, while there is also an internal abundance spread in And III, it is low compared to most other dSph galaxies.

The variable star content of And I was initially investigated

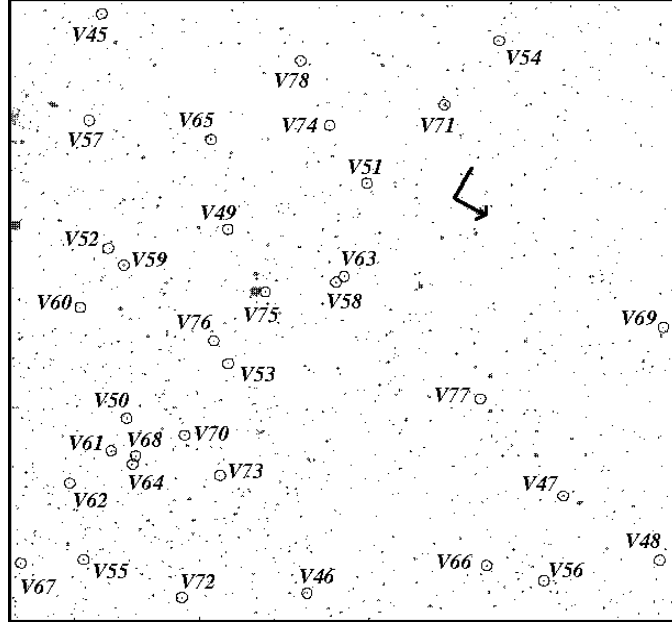


FIG. 2 CONT.— Finding charts for the And I variable stars. The WFC2 ($1.2' \times 1.3'$), WFC3 ($1.3' \times 1.2'$), and WFC4 ($1.2' \times 1.2'$) images are each shown in a panel. North and east directions are shown with the arrow pointing toward the north.

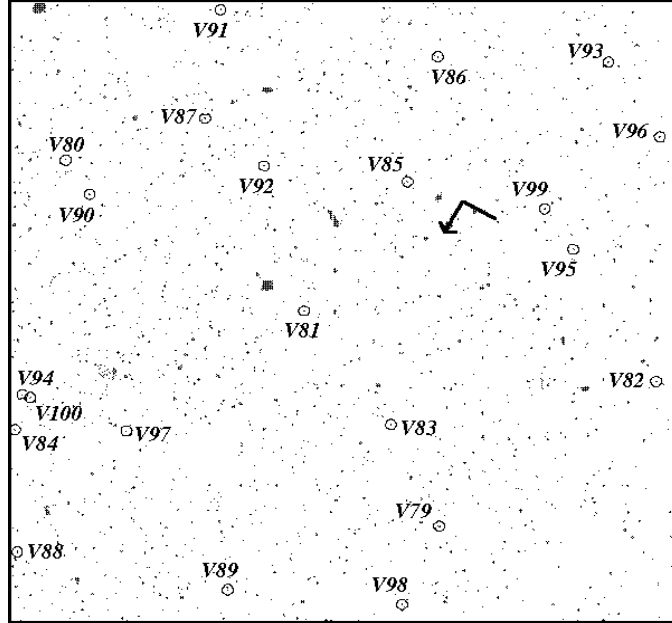


FIG. 2 CONT.— Finding charts for the And I variable stars. The WFC2 ($1.2' \times 1.3'$), WFC3 ($1.3' \times 1.2'$), and WFC4 ($1.2' \times 1.2'$) images are each shown in a panel. North and east directions are shown with the arrow pointing toward the north.

in DACS96 and later in more detail in Da Costa et al. (1997), while that for And III was investigated in DAC02. In this paper we expand upon those works bringing to bear the techniques described below and in Paper I. After describing the processing of the data, we discuss the variable star contents of these galaxies and compare them with those for other dSph galaxies. We also discuss how the variable star populations reflect the properties of And I and And III.

2. OBSERVATIONS AND REDUCTIONS

Observations of And I were taken by the HST/WFPC2 as part of the GO Program 5325 on 1994 August 11 and 16, us-

ing the same orientation. Three 1800 s integrations through the F555W filter and six 1800 s integrations through the F450W filter were taken in the first set of observations. Identical exposure times were used for the second set of observations, but there were four F555W and six F450W integrations.

For And III, the observations were taken for the GO Program 7500 on 1999 February 22 and 26 with the same orientation. Each set of observations had four observations of 1200 s in F555W and eight observations of 1300 s in F450W. As for And I, the two sets of observations were slightly offset from each other to minimize the impact of instrumental defects. For And III, the field center was offset from the center

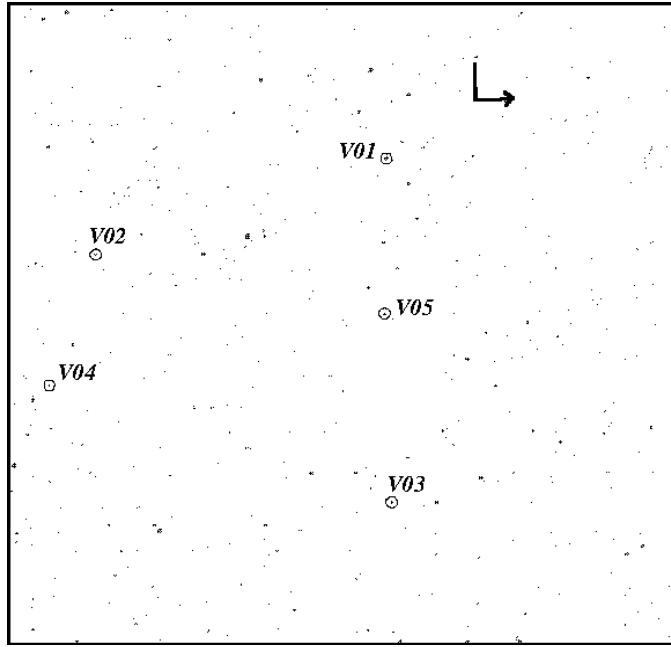


FIG. 3.— Finding charts for the And III variable stars. The PC ($0.5' \times 0.5'$), WFC2 ($1.2' \times 1.3'$), WFC3 ($1.3' \times 1.2'$), and WFC4 ($1.2' \times 1.2'$) images are each shown in a panel. North and east directions are shown with the arrow pointing toward the north.

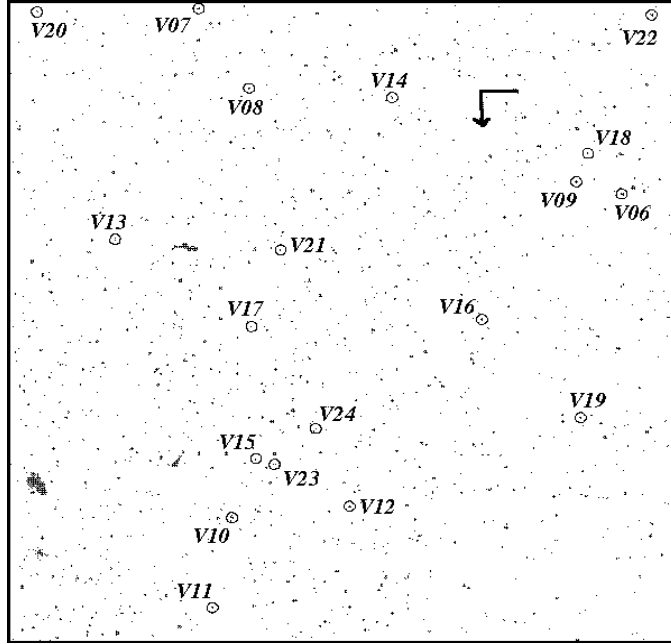


FIG. 3 CONT.— Finding charts for the And III variable stars. The PC ($0.5' \times 0.5'$), WFC2 ($1.2' \times 1.3'$), WFC3 ($1.3' \times 1.2'$), and WFC4 ($1.2' \times 1.2'$) images are each shown in a panel. North and east directions are shown with the arrow pointing toward the north.

of the dSph galaxy to avoid bright foreground stars (see Fig. 1 of DAC02).

The point-spread function fitting photometry was performed with ALLFRAME (Stetson 1994) as described in Paper I. Similarly, the aperture and charge-transfer efficiency corrections along with the B, V calibrations were carried out in the same fashion. As with And II, we have the photometry used in creating the color-magnitude diagrams (CMDs) so we may compare our photometry with that of DACS00 and DAC02. We list in Table 1 the mean differences between the two sets of photometry. There are obvious systematic dif-

ferences that are of similar size and sign as those found for And II in Paper II. The origin of these systematic differences is unclear, although it likely is due to the different techniques and calibration processes. Fortunately they appear to be just zero point offsets: there is no dependence of these differences on magnitude. We have applied them to our data in order to keep the present photometry consistent with the earlier work. It should also be noted that DAC02 found their HST V -band photometry to be consistent with ground-based observations of And III.

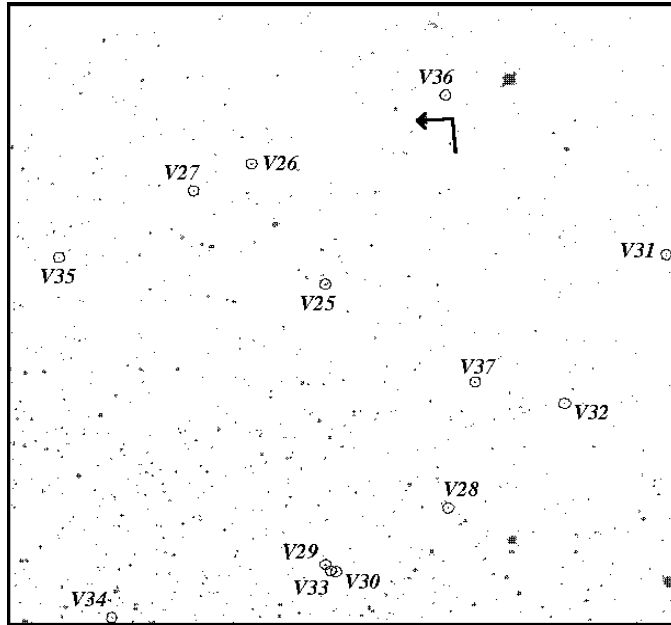


FIG. 3 CONT.— Finding charts for the And III variable stars. The PC, (0.5' x 0.5'), WFC2 (1.2' x 1.3'), WFC3 (1.3' x 1.2'), and WFC4 (1.2' x 1.2') images are each shown in a panel. North and east directions are shown with the arrow pointing toward the north.

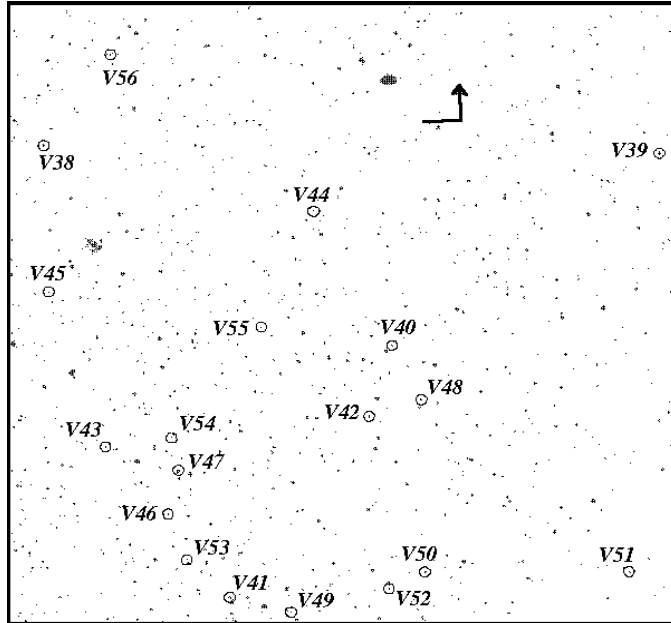


FIG. 3 CONT.— Finding charts for the And III variable stars. The PC (0.5' x 0.5'), WFC2 (1.2' x 1.3'), WFC3 (1.3' x 1.2'), and WFC4 (1.2' x 1.2') images are each shown in a panel. North and east directions are shown with the arrow pointing toward the north.

3. VARIABLE STARS

As was done in Papers I and II, the photometry of the individual images was searched for variable stars using DAOMASTER, a routine created by P. B. Stetson. DAOMASTER compares the rms scatter in the photometric values with that expected from the photometric errors returned by the ALL-FRAME program. For And I, we do not include the PC data since only a small number of RR Lyrae (RRL) stars were found and no candidate anomalous Cepheids (ACs). On the other hand, we did find one AC on the PC for And III. Therefore we include the RRL stars found on that chip in our analysis. Period searches of the variable stars were done using the

routines created by A. C. Layden as outlined in Papers I and II. The routines determine the most likely period from the χ^2 minima by fitting the photometry of the variable star with 10 templates over a selected range of periods. A cubic spline was fitted to each template light curve to determine the mean magnitudes and colors. The amplitudes derive from the template fits.

As discussed in Paper I, the nature of the observations makes the determination of precise periods and magnitudes a challenge. The data for both filters are combined to allow for more accurate magnitudes and periods (see Paper I for more details). As was done in the previous papers in this series,

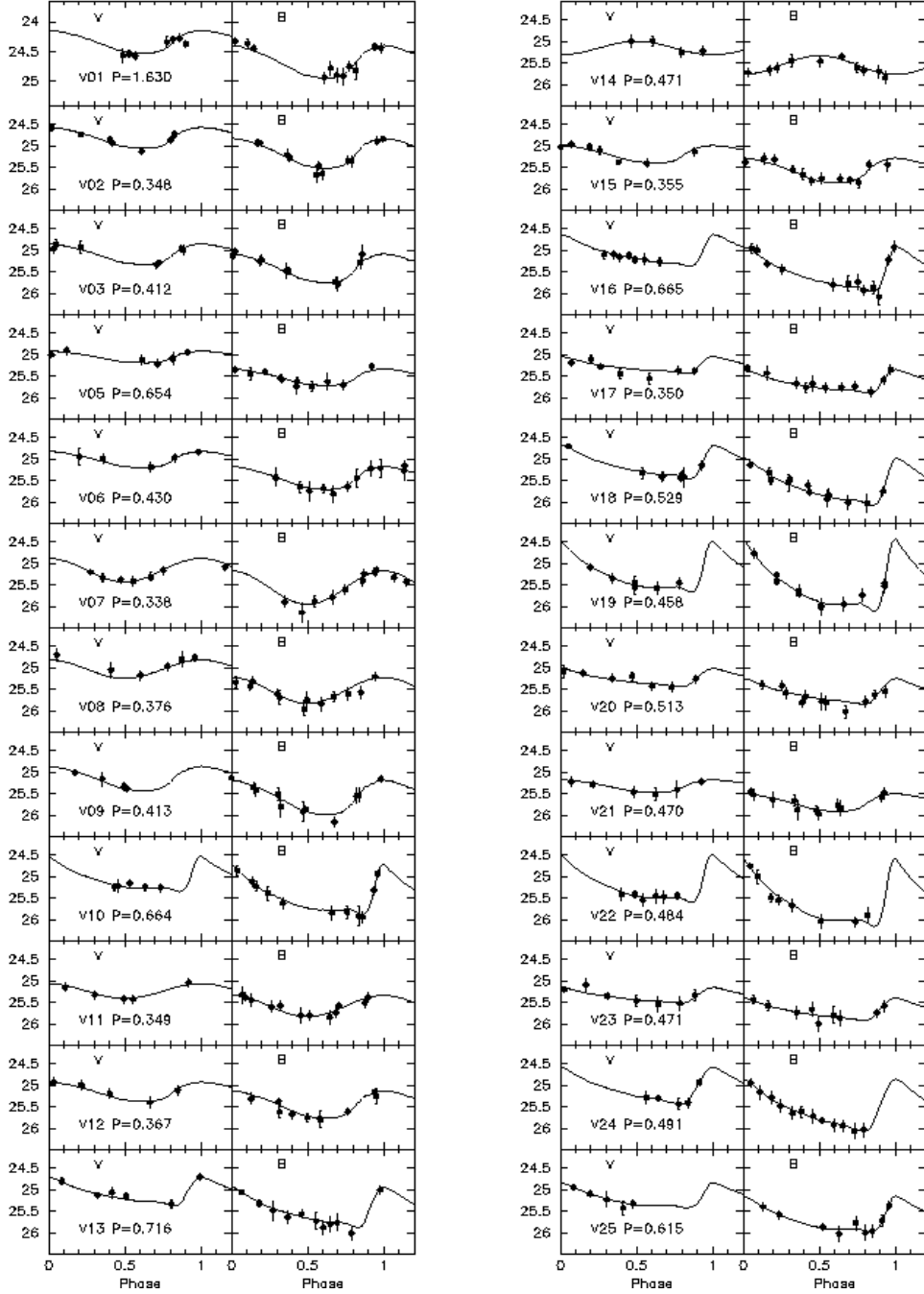


FIG. 4.— And I variable star light curves. The observations are shown as filled circles and the fitted templates are displayed as curves.

we used the period-amplitude diagram to test the periods of the RRL stars. When one of these stars was scattered from the majority in the period-amplitude diagram we revised the period to reduce the scatter. Although there is a slight possibility that a small number of And I and And III RRL stars may have an alias period, the combination of the template-fitting program and the period-amplitude diagram reduces the likelihood of this happening.

Figure 1 shows the CMDs of DACS00 (And I) and DAC02 (And III) in which we have replaced their photometry with that derived here for all the stars found to be variable in our survey. Further, we checked all the DACS00 and DAC02 stars

in Figure 1 that fall in the region of the instability strip along the HB or brighter for variability. However, no additional variables were found. Each variable is plotted according to its intensity-weighted $\langle V \rangle$ magnitude and magnitude-weighted $(B-V)$ color. Table 2 lists the photometric data for the variable stars in And I, while Table 3 lists these for And III. For both tables, column 1 lists the star's ID, while the next two columns give the RA and Dec. Column 4 lists the period of each star. The intensity-weighted $\langle V \rangle$ and $\langle B \rangle$ magnitudes along with the magnitude-weighted colors $(B-V)_{\text{mag}}$ are shown in columns 5 - 7. Columns 8 and 9 give the V and B amplitudes of the variable stars. The classifications of the variable stars

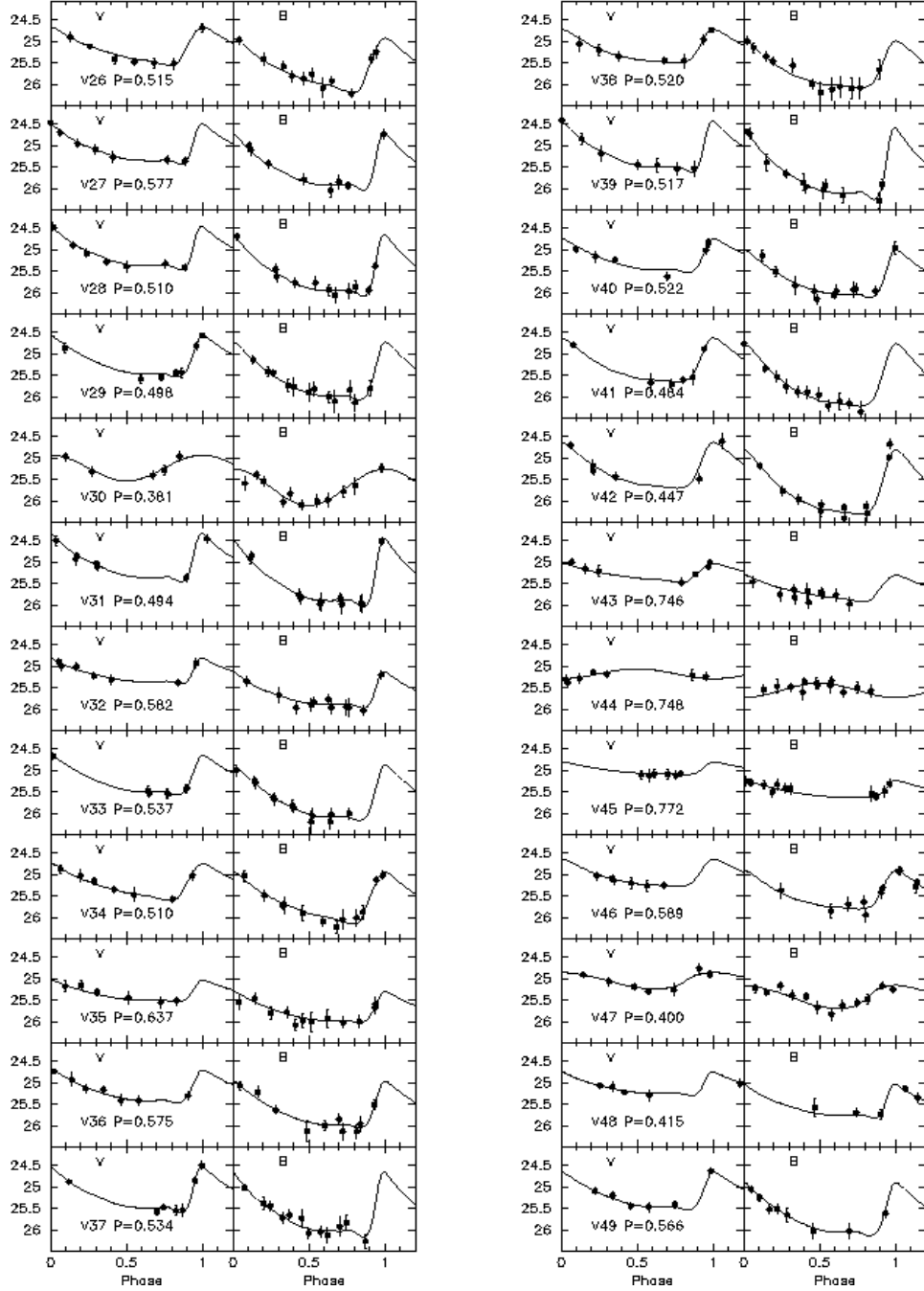


FIG. 4 CONT.— And I variable star light curves. The observations are shown as filled circles and the fitted templates are displayed as curves.

are listed in column 12. The remaining columns will be discussed later in the paper. Figures 2 and 3 are the finding charts for And I and And III, respectively, while Tables 4 - 7 give the photometric B and V data for And I and And III. The light curves for the variable stars in And I are shown in Figure 4, while those for And III are in Figure 5.

For And I, there is one clear supra-HB variable star in the CMD (Fig. 1a). This star may be a Population II Cepheid (P2C) and is discussed in the following section. There are also two variable stars that are clearly fainter than the HB. These stars will be discussed in §5.1.1.

The And III CMD in Fig. 1b shows five variable stars

brighter than the RRL along the HB. DAC02 discovered two of these stars and suggested one (V08=WF2-1398 in DAC02) may be a P2C. This possibility is also discussed in the next section. The two CMDs also show that And III, despite having a lower mean metallicity than And I, has a redder HB (cf. DAC02).

4. ANOMALOUS CEPHEIDS AND POPULATION II CEPHEIDS

As mentioned above, And I has one supra-HB variable star and And III has five. Following the prescription used in Paper I, we list the absolute magnitudes for these stars in Table 8 assuming a distance modulus and visual absorption of 24.49 ± 0.06 mag and 0.16 ± 0.03 for And I (DACS00) and

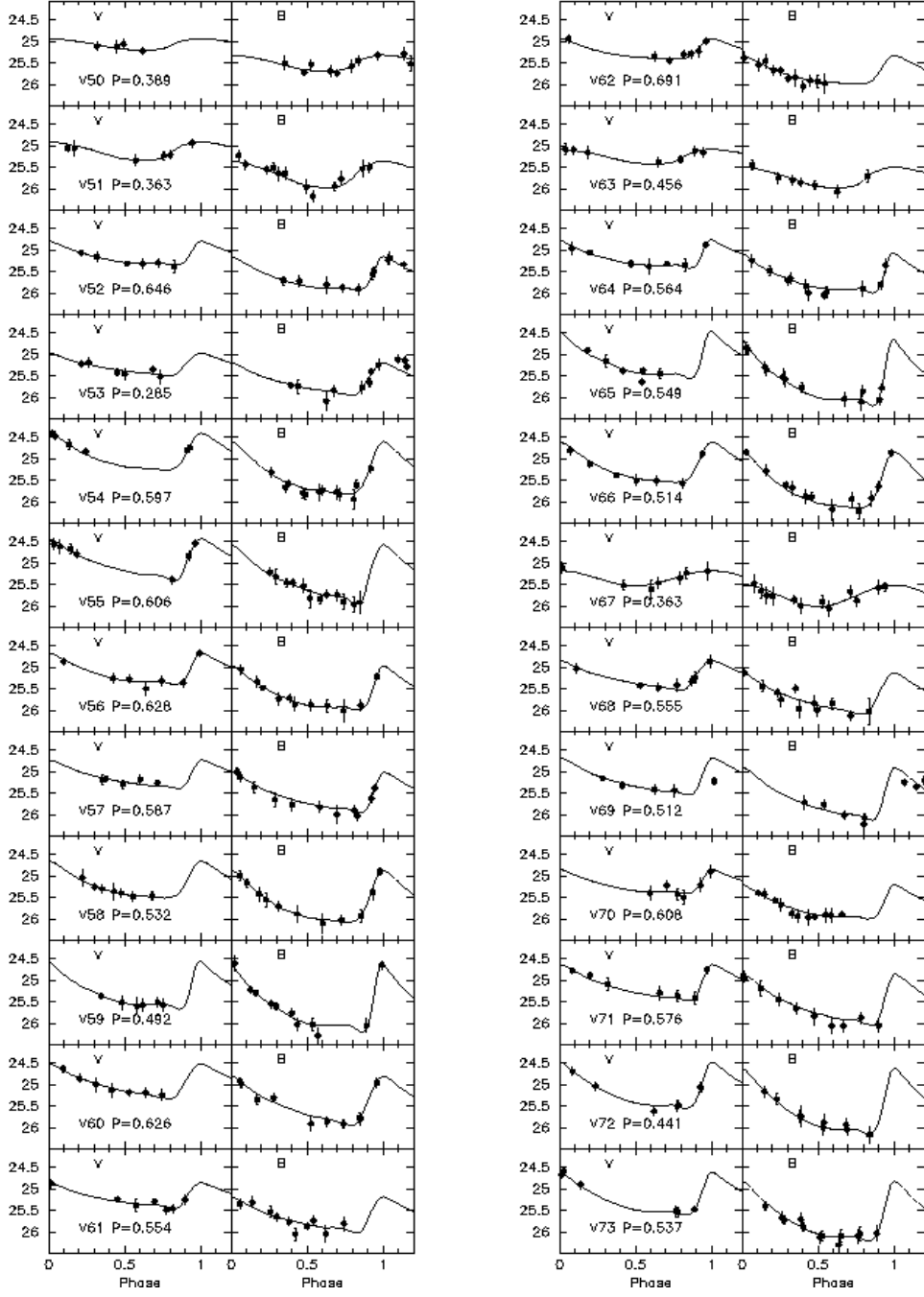


FIG. 4 CONT.— And I variable star light curves. The observations are shown as filled circles and the fitted templates are displayed as curves.

24.38 ± 0.06 mag and 0.17 ± 0.03 for And III (DAC02). The period-luminosity relation shown in Figure 6 plots the ACs from Paper I and Paper II along with the supra-HB variable stars in And I and And III. Four of the supra-HB variable stars in And III fit in well with the other ACs in this Figure confirming their classification as ACs. These ACs are also found to be consistent with the other ACs in a period-amplitude diagram.

In addition to the AC period-luminosity (P-L) relation lines, we plot in Figure 6 the P2C P-L relation for $P < 10$ days using equation 11 in McNamara (1995). Clearly, V01 in And I and V08 in And III fall near the P2C line for their given magnitude and period. The way the data were taken and the rela-

tively long apparent periods for these stars combine to generate significant gaps in their light curves. This leads to higher uncertainty in their periods and magnitudes compared to the rest of our data. If V01 in And I is a P2C, then it will mean that we have been unable to find a definite AC in this dSph galaxy. And I might then become the first dSph galaxy without an AC, though we have not by any means surveyed all of the galaxy for variable stars (see Table 9). We also note, as was first shown by DAC02 using a different “shorter” period, that it is possible to fit the observations for And III V08 with a period as short as $P = 0.655$ d. This would make the star an AC, although this is not the best χ^2 fit according to

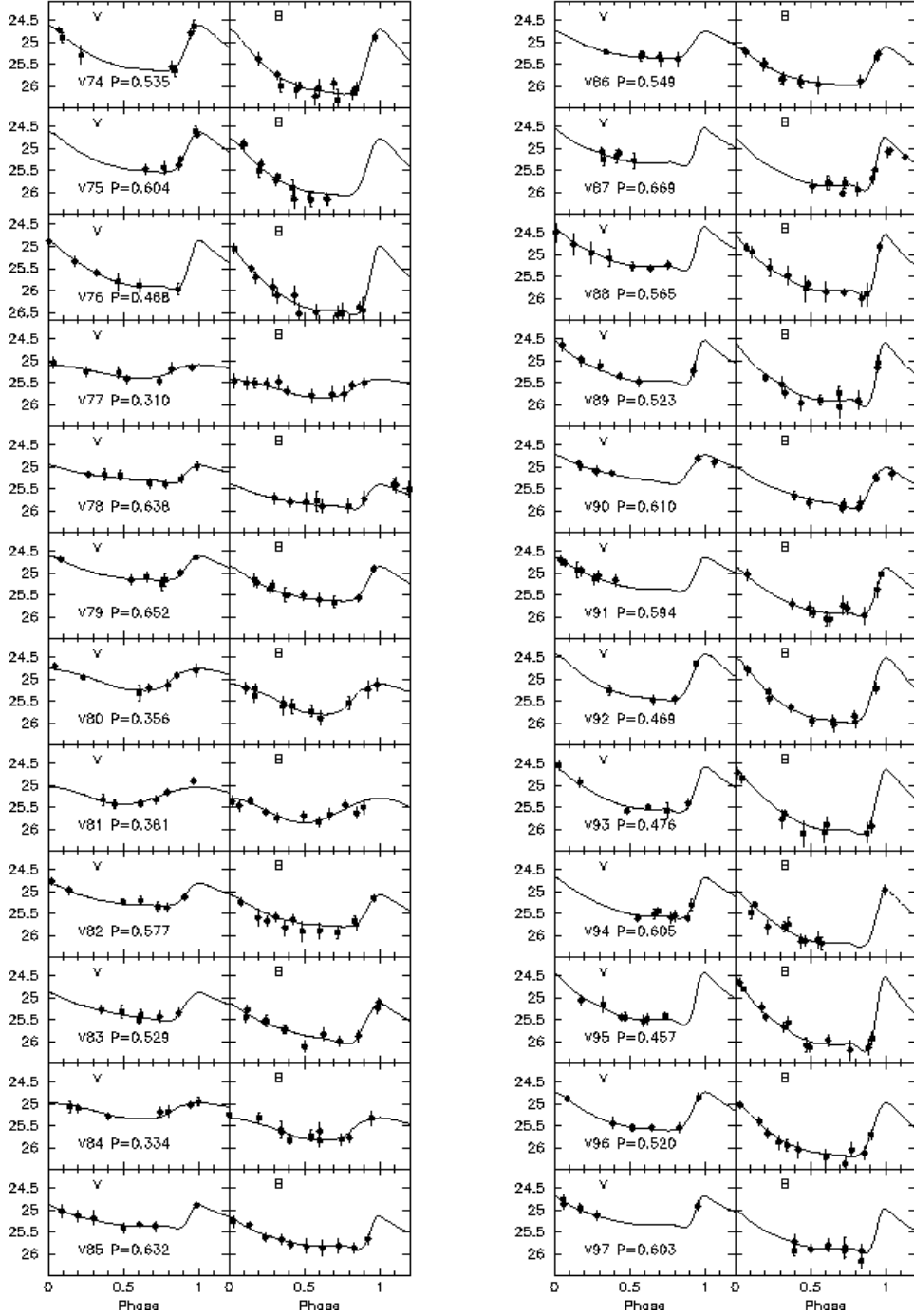


FIG. 4 CONT.— And I variable star light curves. The observations are shown as filled circles and the fitted templates are displayed as curves.

the template fitting program we have employed. Given the lack of phase coverage, we do not feel comfortable forcing a change in the period solely to make it an AC. The mean magnitudes we find for this short period would place the variable on the fundamental mode period-luminosity relation line for the ACs. We were unable to find a viable “AC-like” period for And I V01.

Do we expect to see P2C variables in dSph galaxies? In Galactic globular clusters, the main property associated with the presence of P2Cs are strong blue HBs (e.g., DAC02; Wallerstein 2002). In particular, the shorter period P2Cs,

known as BL Her stars, which And I V01 and And III V08 would be classified as, are assumed to be post blue HB stars evolving through the instability strip towards the asymptotic giant branch. Of the Galactic dSph galaxies, only Fornax has been shown to contain P2Cs (Bersier & Wood 2002). It may be that Fornax has a significant population of blue HB stars that could provide a source for P2Cs, but it is difficult to infer this from the CMD as the blue HB region is severely contaminated by main sequence stars. On the other hand, the CMDs for And I and And III clearly do not contain strong blue HB populations (see Figure 1) and this would seem to argue

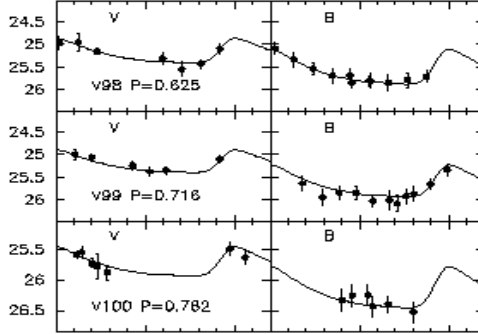


FIG. 4 CONT.— And I variable star light curves. The observations are shown as filled circles and the fitted templates are displayed as curves.

against the P2C interpretation. We are forced to conclude that further observations of these stars are needed to clarify their periods and light curve shapes, and thus their classification.

4.1. The Frequency of Anomalous Cepheids in dSph Galaxies

Mateo et al. (1995) pointed out that the specific frequency of ACs (the number of ACs per $10^5 L_{V,\odot}$) correlates with both (visual) luminosity and mean abundance for the Galactic dSphs. In Paper II we updated the Galactic dSph data and found that the M31 dSphs And II and And VI apparently follow the same correlations. We now explore whether this result applies also to And I and And III. In Table 9 we list the data used in calculating the specific frequency of ACs for And I and And III (cf. Table 5 of Paper II). We note that in this discussion, the supra-HB variable stars in And I and And III that may be ACs or P2Cs, have been assumed to be ACs. Without this assumption, And I would have no ACs and And III would have a specific frequency of 1.7 per $10^5 L_{V,\odot}$. Figure 7 plots the logarithm of specific frequency against M_V and mean metallicity for And I and And III along with the data from Paper II. We also include the specific frequency value for the Phoenix dwarf irregular galaxy from Gallart et al. (2004). Clearly, like And II and And VI (cf. Paper II), And I and III fall near the line defined by the Galactic dSph galaxies, as does Phoenix (cf. Gallart et al. 2004). Consequently, it appears that the correlation between AC specific frequency and either (visual) luminosity or metallicity seen in the Galactic dSph galaxies applies also to the M31 systems.

As pointed out by Mateo et al. (1995) and in Paper II, it is perhaps surprising to see a strong correlation between the specific frequency of ACs and the total luminosity of the dSph galaxies given the stellar population differences among the dSphs, and the fact that there are two different mechanisms that can create ACs, one from younger stars and the other from mass-transfer in binaries. Both mechanisms are complicated and both can occur in a dSph galaxy, as discussed by Bono et al. (1997) using various stellar models. However, as noted by Mateo et al. (1995) and in Paper II, the mean abundances of dSph galaxies are well correlated with their luminosities, with the lower luminosity systems having lower abundances. Thus, since regardless of the mechanism creating the AC the star needs to be metal-poor to enter the instability strip, it may simply be that it is easier to generate ACs in a more metal-poor environment.

We now comment briefly on the observed lack of ACs in the M31 halo field surveyed for variable stars by Brown et al. (2004). Given the results of Durrell, Harris, & Pritchett (2004), for example, we can assume that the mean metallicity

for the surveyed region is approximately $\langle [\text{Fe}/\text{H}] \rangle = -0.8$. Then assuming that the relation between AC specific frequency and mean abundance shown in Figure 7 can be extended to mean abundances of this order, the linear fit shown gives $\log S \sim -1.55$ per $10^5 L_V$. The mean surface brightness and area of the region (Brown et al. 2004), then yield, assuming $(m - M)_V = 24.5 \pm 0.1$ mag, a visual luminosity for the region of $7.4 \times 10^5 L_V$. Therefore, the number of ACs expected in the field is ~ 0.2 . This is certainly consistent with the fact that Brown et al. (2004) found none. However, we know that ACs derive from metal-poor stellar populations ($[\text{Fe}/\text{H}] < -1.3$; Demarque & Hirshfeld 1975). Consequently, using a mean metallicity of $[\text{Fe}/\text{H}] = -0.8$ may not be the most appropriate approach. Using Eq. 2 of Alcock et al. (2000), Brown et al. (2004) found that the RRL population in their field has a mean metallicity of -1.79 . For this metallicity, Figure 7 gives $\log S \sim -0.1$ per $10^5 L_V$. However, in this situation, we cannot apply the total visual luminosity for the surveyed region. Brown et al. (2003) argue that, in this region, the old, metal-poor stellar population makes up at most 30% of the total (cf. Durrell et al. 2004). Scaling the total luminosity by this fraction then predicts 1.8 ACs in the surveyed field. This number is not inconsistent with the observed lack of ACs given small number statistics and the uncertainty in the luminosity fraction generated by the metal-poor population. Clearly further variable star searches over larger areas are required to more fully investigate whether or not ACs exist in the M31 halo. A confirmed lack of such stars would add strength to the contention that the disruption of dwarf galaxies comparable to the existing M31 dSph companions was not a major contributor to the build-up of the M31 halo.

4.2. Anomalous Cepheids = Short-Period Cepheids?

Recently, the number of variable star surveys of dwarf galaxies has increased, especially for dwarf irregular galaxies such as IC 1613 (Dolphin et al. 2001), Leo A (Dolphin et al. 2002), Sextans A (Dolphin et al. 2003), NGC 6822 (Clementini et al. 2003) and Phoenix (Gallart et al. 2004). These studies have revealed a number of short-period (Classical) Cepheids. Given that these variables have periods similar to the ACs and comparable magnitudes, there is some question as to the distinction between the two classes of variables. Using the OGLE Small Magellanic Cloud database (Udalski et al. 1999), Dolphin et al. (2002) found the P-L relations for Cepheids with periods of two days or less was similar to the AC P-L relations of Nemec, Nemec, & Lutz (1994). Therefore, they concluded that there was no clear distinction between ACs and short-period Cepheids in terms of their posi-

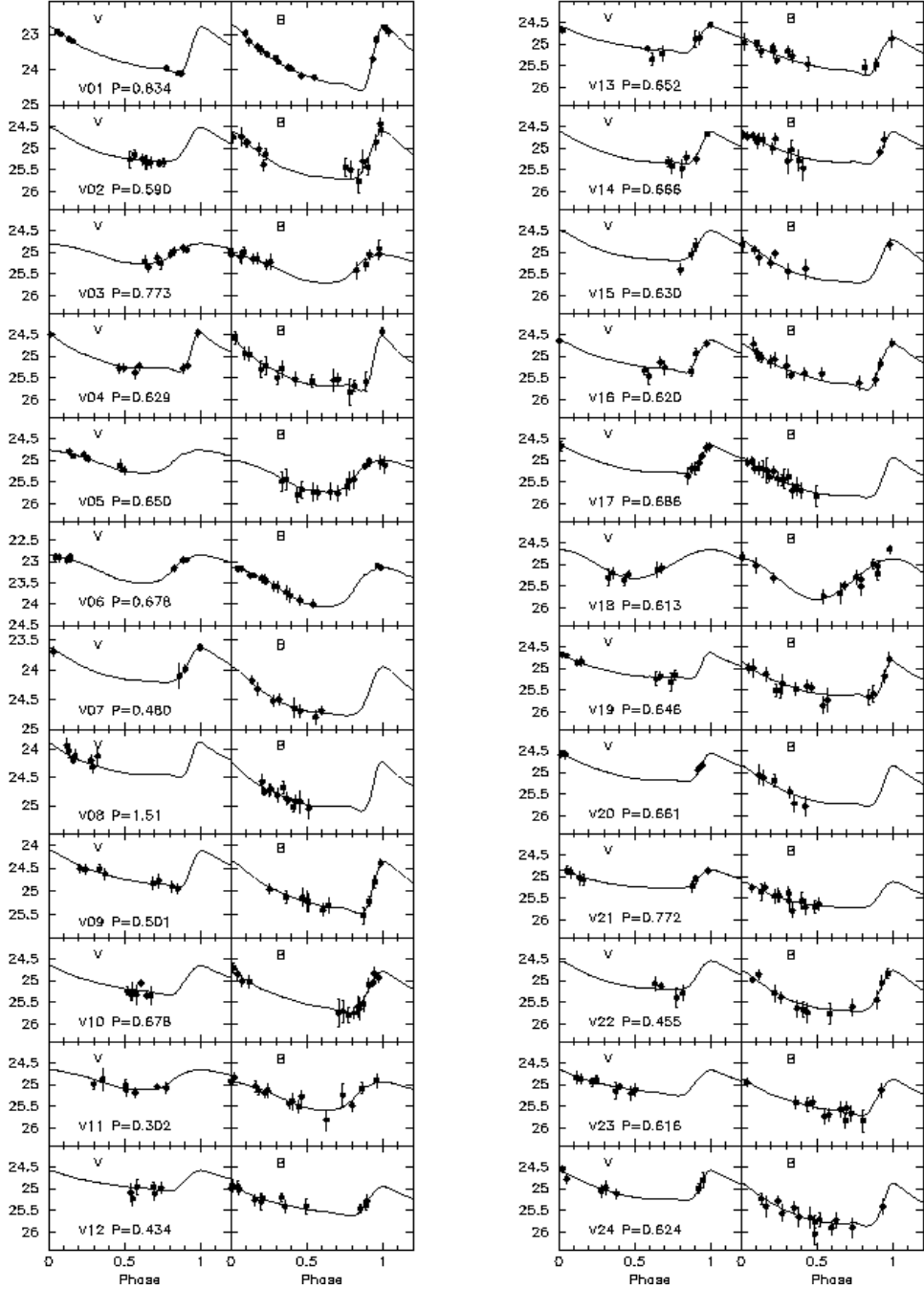


FIG. 5.— And III variable star light curves. The observations are shown as filled circles and the fitted templates are displayed as curves.

tion in the P-L relations. The only difference between these two classes would be that short-period Cepheids are predominantly found in systems with young stars (ages < 100 Myr) while ACs preferentially occur in systems that lack such young stars.

Baldacci et al. (2003) were the first to show that the short-period Cepheids in dwarf irregular galaxies, including the Large and Small Magellanic Clouds, have P-L relations different than those of ACs as given in Paper I. They also comment that Phoenix and NGC 6822 may have their instability strip continuously populated from the RRL stars, through the ACs to the short-period Cepheids. Marconi, Fiorentino, & Caputo

(2004) and Gallart et al. (2004) took this a step further claiming that some of the short-period Cepheids in dwarf galaxies such as Leo A and Sextans A may actually be ACs.

Following the same method as outlined in §4 of Paper I, we determined the absolute magnitudes of the short-period Cepheids in IC 1613, Leo A, and Sextans A using the tip of the red giant branch as the distance indicator. This is to ensure consistency between the absolute magnitudes found for the ACs and the short-period Cepheids. We plot the absolute magnitude of the short-period Cepheids against their periods in Figure 8 along with the lines for the AC P-L relations as determined in Paper I (cf. Eqns. 4 and 5). Looking first at

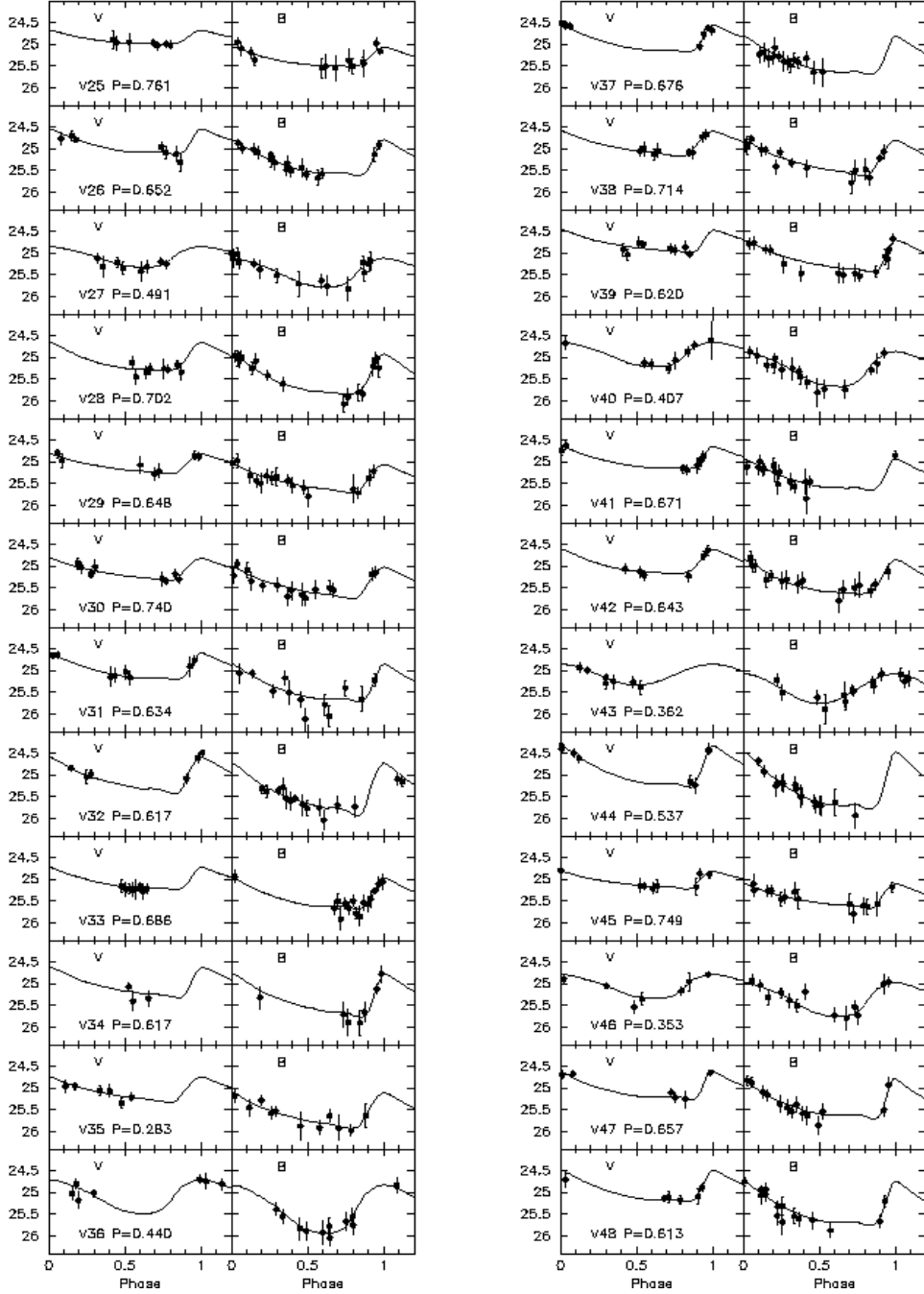


FIG. 5 CONT.— And III variable star light curves. The observations are shown as filled circles and the fitted templates are displayed as curves.

the fundamental mode variables, which are found at a fainter magnitude than the first-overtone variables for a given period, the short-period Cepheids are clearly found at higher luminosity than the ACs at a given period. For the first-overtone Cepheids, the case isn't as clear. However for a set period, these stars are still offset toward brighter absolute magnitudes than the first-overtone ACs, especially at short periods. There are some stars which are located near the AC P-L lines, but this may be due to the uncertainties in the periods and magnitudes of the stars. The higher luminosity at fixed period for the short-period Cepheids relative to the ACs indicates that these stars have higher masses than the ACs. This is not unex-

pected given that these dwarf irregular galaxies have on-going star formation which the dSph galaxies lack.

Our analysis agrees with Baldacci et al. (2003), Marconi et al. (2004), and Gallart et al. (2004) as regards to the existence of a difference between the P-L relations for ACs and short-period Cepheids. In essence, the reason we do not see as many short-period Cepheids lying along the AC P-L relations as do Dolphin et al. (2001, 2002, 2003) lies with their use of the Nemec, Nemec, & Lutz (1994) AC P-L relations rather than those of Paper I. This does not mean, however, that dwarf galaxies such as Leo A and Sextans A do not contain both short-period and anomalous Cepheids. Indeed, we

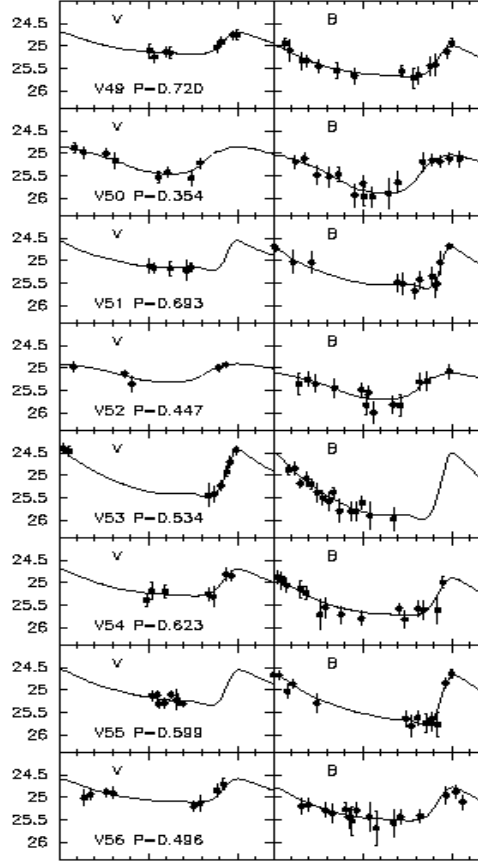


FIG. 5 CONT.—And III variable star light curves. The observations are shown as filled circles and the fitted templates are displayed as curves.

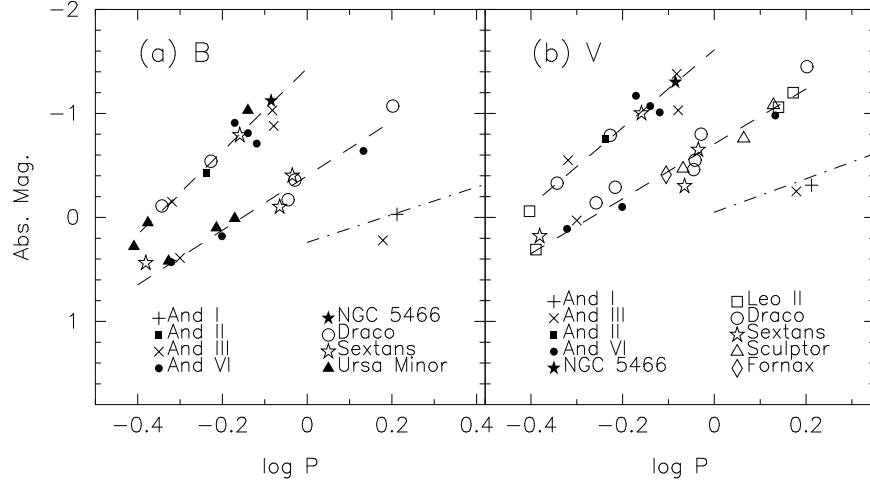


FIG. 6.—Period-luminosity diagrams for anomalous Cepheids for both the (a) B and (b) V filters. The anomalous Cepheid fundamental and first-overtone mode period-luminosity relations from Pritzl et al. (2002) are shown as dashed lines. The Population II Cepheid period-luminosity line from McNamara (1995) is shown as a dotted-dashed line.

encourage further observations of these and other dwarf irregular galaxies to search for such stars.

5. RR LYRAE STARS

5.1. *And I*

We detected 99 RRL stars in our field-of-view of And I, with 72 pulsating in the fundamental mode (RRab) and 26 pulsating in the first-overtone mode (RRc). This nearly doubles the number of RRL stars found by Da Costa et al. (1997),

who detected 50 RRL stars. One variable, V04, remains unclassified due to a lack of F555W data because of a chip defect. It is likely an RRL star given its F450W magnitude. The presence of the RRL stars indicates that And I contains a stellar population with an age > 10 Gyr. It should be noted that due to the low amplitudes of the RRc stars, we may not have detected all of the possible stars pulsating in this mode.

We find the mean period of the And I RRab and RRc stars to be 0.575 day and 0.388 day, respectively. The ratio of RRc

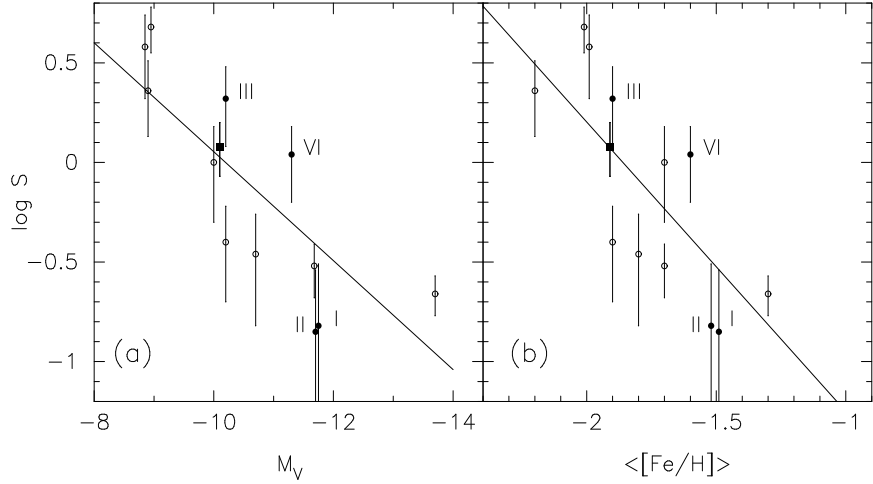


FIG. 7.— Specific frequency of anomalous Cepheids in dwarf spheroidal galaxies as a function of the absolute visual magnitude (left panel), and the mean metallicity of the dwarf galaxy (right panel). The Galactic dwarf spheroidal galaxies are shown as open circles, while the M31 ones are shown as filled circles. The Phoenix dwarf galaxy is shown as a filled square. In both plots, there are clear trends that the Galactic dwarf spheroidal galaxies follow as shown by the least squares fit to the data. The M31 dSph galaxies follow these trends, including And I and And III. Note that we have assumed that the two supra-HB variables stars And I V01 and And III V08 to be anomalous Cepheids, although their classification is uncertain.

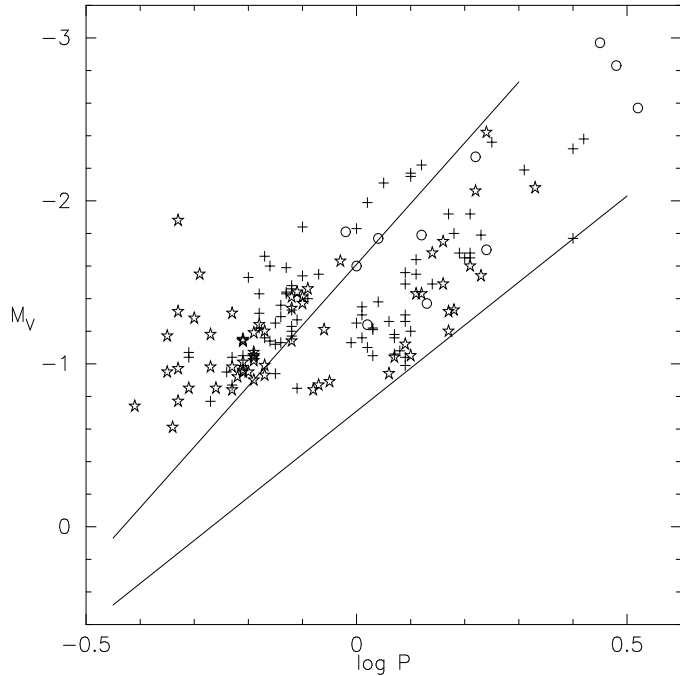


FIG. 8.— V -band absolute magnitude versus the logarithm of the period for short period Cepheids in Sextans A (plusses), IC 1613 (open circles), and Leo A (open stars). The solid lines are the period-luminosity relations representing the fundamental and first-overtone mode anomalous Cepheids (Pritzl et al. 2002). This plot clearly illustrates that the short period Cepheids are found at higher luminosities than the anomalous Cepheids at a given period.

stars to the total number of RRLs, N_c/N_{RR} , is 0.27. If we place these values in Table 6 of Paper I according to the metallicity given in DACS00, $\langle \text{[Fe/H]} \rangle = -1.46 \pm 0.12$, we find that they are consistent with those found for other dSph galaxies. With this metallicity, the RRL stars in And I also follow the mean period - metallicity relation defined by the Galactic globular clusters, as is shown in Figure 9. The mean period for the RRab stars in And I is close to the value found for And II which has a very similar mean metallicity to And I (DACS00). It is interesting to note that this is the case even though there is a large spread among the And II RRab stars in the period-amplitude diagram (see Fig. 7 in Paper II).

The mean magnitude of the And I RRL stars, not in-

cluding the two fainter RRL stars, is found to be $\langle V_{RR} \rangle = 25.14 \pm 0.04$ mag, where the uncertainty is the aperture correction uncertainty, the photometry zeropoint uncertainty in the DAC02 photometry, and the uncertainty in the mean RRL instrumental magnitude derived from the spline-fitting routine added in quadrature to the standard error of the mean. This matches the value determined by DACS00 of $V_{HB} = 25.23 \pm 0.04$ mag. Given $\langle \text{[Fe/H]} \rangle = -1.46 \pm 0.12$, the equation $M_{V,RR} = 0.17[\text{Fe/H}] + 0.82$ from Lee, Demarque, & Zinn (1990) yields $M_{V,RR} = +0.57$ and thus a true distance modulus of 24.42 ± 0.07 mag for the adopted reddening. This corresponds to a distance of 765 ± 25 kpc in good accord with the distance, 790 ± 25 kpc, found by DACS00.

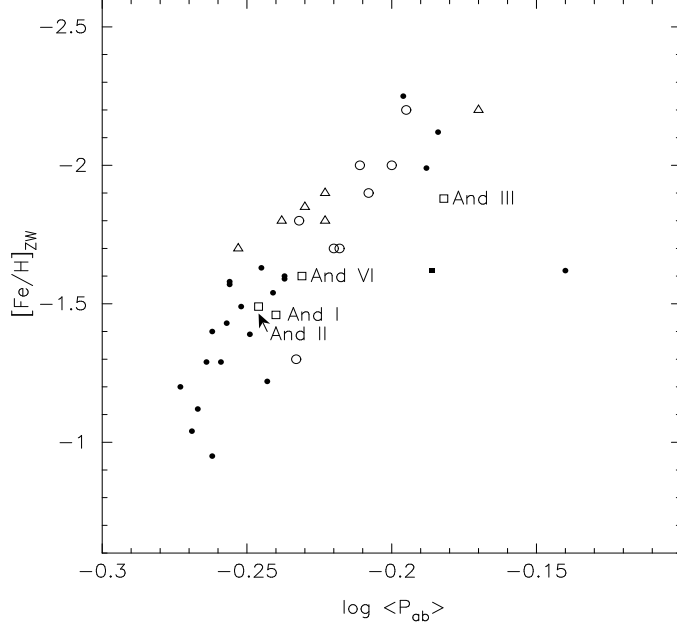


FIG. 9.— Mean period for the RRab stars versus the mean metallicity of the parent system. The Andromeda dwarf spheroidal galaxies are shown as open squares. The Galactic dwarf spheroidals are indicated by open circles. Galactic globular clusters with at least 15 RRab stars are shown as filled circles, along with ω Centauri (filled square). Large Magellanic Cloud globular clusters with a minimum of 15 RRab stars are shown as open triangles.

5.1.1. M31 Halo RR Lyrae Stars?

According to DACS96 and DACS00, the line-of-sight distance between M31 and And I is 0 ± 70 kpc and the true distance of And I from the center of M31 is somewhere between ~ 45 and ~ 85 kpc. This makes And I the closest dSph to M31 leading to the possibility that there may be contamination of the CMD from M31 halo stars. In fact, DACS96 showed that a number of stars somewhat fainter and redder than the And I red giant branch (RGB) in their CMD were likely to be from the M31 halo.

Variable stars V76 and V100 in And I are both clearly fainter than the rest of the RRL in this dSph galaxy. We checked the images for any defects near these stars which may have affected their photometry and none were found. DACS96 drew attention to a population of faint blue stars in And I which they suggested might be blue straggler stars analogous to those found in globular clusters. Some blue straggler stars are known to be short period variables (δ Scuti), but the periods of the And I faint variables are too long for them to be interpreted in this way. Therefore, it appears that V76 and V100 must originate from a stellar population not associated with And I. The only logical interpretation of this is that they are part of the M31 halo.

We can attempt to verify this assertion by making use of the recent study of RRL stars in the halo of M31 of Brown et al. (2004). These authors used the Advanced Camera for Surveys on HST to provide a complete census of RRL stars in a halo field approximately 51 arcmin from the center of M31 on the minor axis. In their field the density of RRab variables is 2.24 per arcmin². Brown et al. (2004) also give the surface brightness of the M31 halo at the location of their field as 26.3 V mag per arcsec². Using the Pritchett & van den Bergh (1994) surface brightness profile, DACS96 estimated the M31 halo surface brightness in the vicinity of And I as approximately 29.5 V mag per arcsec². Then assuming no change in the stellar population with radius, these figures imply a M31

halo RRab density at the location of And I of approximately 0.12 per arcmin². Combined with the area of the field studied here, this density predicts only 0.6 M31 halo RRab should be present in our data, rather than the two observed. Consequently, even allowing for small number statistics, it appears that these two fainter RRL may be associated with a region of moderately enhanced density in the halo of M31. This conclusion is strengthened by looking at the magnitude distribution of the RRab stars in the Brown et al. (2004) M31 halo field. The 29 stars have a mean V magnitude, corrected to the reddening of the And I, of $\langle V \rangle = 25.18$ mag, with a standard deviation of 0.11 mag (in F606W, which for this purpose we can equate with σ_V). The largest excursion from this mean on the faint side is only 0.24 mag. Consequently, the two fainter RRab stars in the And I field are both more than 3σ fainter than the mean, increasing the likelihood that they are associated with a distinct feature, rather than the general field in the outer halo of M31.

This indeed may be the case. McConnachie et al. (2003) have used the CHF12k CCD mosaic camera to map the giant stellar stream in the halo of M31 (Ibata et al. 2001; Ferguson et al. 2002) to larger radial distances. They find the stream extends to the South-East of M31 for at least 4.5° , and using the tip of the red giant branch as a distance indicator, McConnachie et al. demonstrate that the Stream is on the far side of M31, increasingly so as the angular distance from M31 increases. Coincidentally, And I is projected close to this Stream on the sky, and, based on Fig. 7 of McConnachie et al., we estimate that the Stream lies approximately 150 kpc beyond M31 (and And I, which is at the same distance as M31 [DAG02]) at the location of And I. This corresponds to a total distance of ~ 875 kpc or an apparent visual distance modulus of approximately 24.9 mag. If the two faint RRL stars are members of this Stream, then their absolute visual magnitudes would be ~ 0.7 (V76) and ~ 0.9 (V100). Such values are not unexpected given the apparent metal-rich nature of the Stream (Ibata et al. 2001; Ferguson et al. 2002; McConnachie et al.

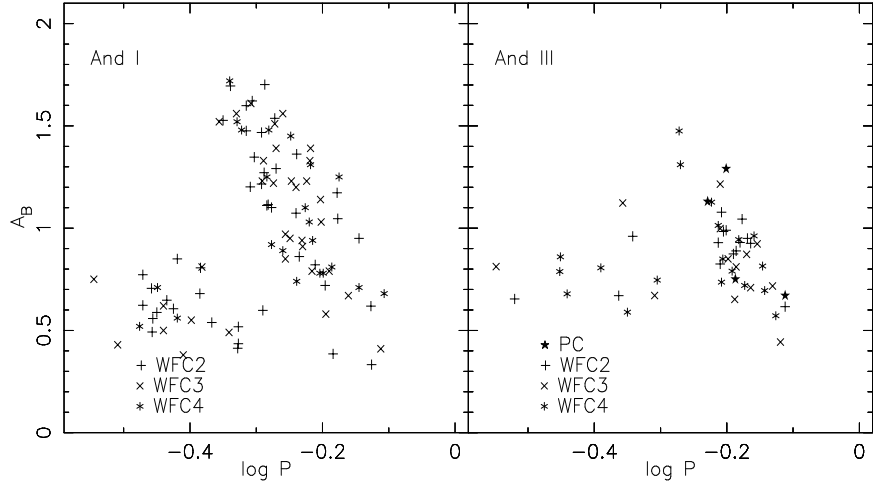


FIG. 10.— Period-amplitude diagram for the RR Lyrae stars in And I (left panel) and And III (right panel) for the B filter.

2003). We conclude then that it is quite possible that the two faint RRL stars observed in the field of And I are associated with the recently identified Stream in the halo of M31, rather than with the general M31 halo field. The existence of RRL stars in the Stream immediately indicates that its progenitor must have contained an old stellar population, and such variables may provide a further means to map both the location of the Stream and to investigate its stellar population.

5.2. And III

For And III, we found a total of 51 RRL, 39 pulsating in the fundamental mode and 12 in the first-overtone mode. As mentioned above, it is more difficult to detect the RRc stars due to their smaller amplitudes. Therefore not all of the RRc stars within our field-of-view may have been detected.

The mean periods are 0.657 day and 0.402 day for the RRab and RRc stars, respectively. The N_c/N_{RR} ratio is found to be 0.24, although this number and the mean period for the RRc stars may be uncertain due to undetected RRc stars. As was done above for And I, we can place these values in Table 6 of Paper I according to And III's metallicity of $\langle \text{[Fe/H]} \rangle = -1.88 \pm 0.11$. We find that in comparison to the other dSph galaxies, And III has unusually long periods for its RRab and RRc stars. This can clearly be seen in the mean period - metallicity diagram of Figure 9 where And III lies to the right of the other dSph galaxies and globular clusters with similar abundances. A possible reason for this will be discussed in §5.3.

The mean magnitude for the And III RRL stars is $\langle V_{RR} \rangle = 25.01 \pm 0.04$ mag. DAC02 found the mean V magnitude of the HB of And III to be 25.06 ± 0.04 mag. Given $\langle \text{[Fe/H]} \rangle = -1.88 \pm 0.11$, $E(B-V) = 0.06 \pm 0.01$, and the equations used above, we find $M_{V,RR} = +0.50$ and $A_V = 0.17 \pm 0.03$. This yields a distance of 740 ± 20 kpc, which matches quite well with the estimate of 750 ± 20 kpc by DAC02.

5.3. RR Lyrae Period-Amplitude Diagrams

Figure 10 plots the B -amplitude of the RRL stars against their adopted period for And I and And III. As discussed in Paper I, the scatter in these diagrams was reduced by revising the period of a small number of stars where it was apparent that A. C. Layden's period-finding routines had picked out an

alias of the probable true period. For And I the longer duration of the observation set meant that there were only minimal period revisions for this dSph. Figure 10a also shows that in And I there are a number of longer period RRc stars which overlap with similar period, but higher amplitude, RRab stars.

In Figure 10b, we see that the RRab stars in And III have mostly smaller amplitudes and longer periods. In direct contrast to And I, there is a notable lack of shorter period, higher amplitude RRab stars. It is this lack of shorter period RRab stars that results in a relatively long mean period, thus displacing the And III point in the mean period - metallicity diagram (Figure 9) to the right.

The explanation may lie with the morphology of the horizontal branch in this dSph. It is clear from the CMD of And III (see Fig. 1b; Fig. 3 in DAC02) that the horizontal branch is lacking in stars bluer than the instability strip. A majority of the stars are located toward the red side of the horizontal branch and therefore, more of the red side of the instability strip is filled. As a consequence, longer period RRab and RRc stars are likely. A similar situation is thought to occur for the RRL variables in the globular cluster Ruprecht 106 (Catelan 2004), a cluster which also has a very red HB.

5.4. RR Lyrae Period Shift

Another way to compare the RRL populations is to view their period distribution. In Figure 11 we plot the RRL period distribution for a number of dSph galaxies according to their mean metallicity. As with the mean RRab periods discussed above, there is a trend for the RRab distribution to shift toward shorter periods as the metallicity increases. For And III, the distribution has a marked discontinuity in the RRL numbers at $P \sim 0.6$ day, a further manifestation of the lack of shorter period, higher amplitude RRab stars in this dSph galaxy.

The shift in period among the RRab stars in globular clusters was first noticed by Sandage, Katem, & Sandage (1981) and was later found to be dependent on metallicity by Sandage (1981; 1982a,b). With M3 as the fiducial cluster, the period shifts of RRab stars were determined to follow the relation:

$$\Delta \log P = -(0.129A_B + 0.088 + \log P) \quad (1)$$

by Sandage (1982a,b). Using this equation, Sandage found that more metal-rich globular clusters have $\langle \Delta \log P \rangle \geq -0.01$, while the more metal-poor clusters have $\langle \Delta \log P \rangle \leq$

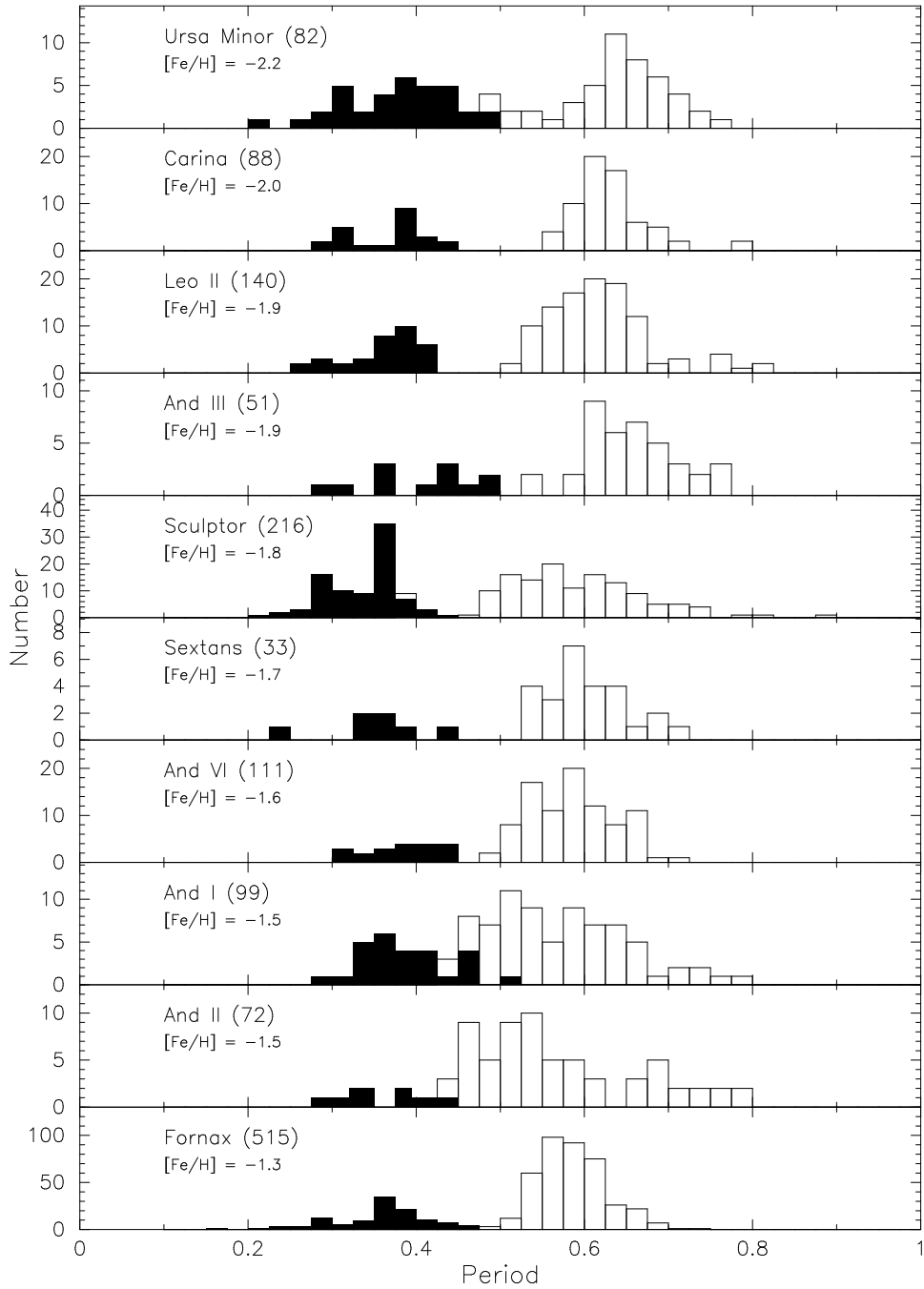


FIG. 11.— Period distribution plots for the RR Lyrae stars in dwarf spheroidal galaxies. The plots are arranged so that the mean metallicity of the parent system increases from the top down. RRab stars are shown as open histograms while RRc stars are shown as filled histograms.

–0.05 with few globular cluster RRab stars found between these values. However, a number of RRab stars in dSph galaxies have been found in this gap (Sextans: Mateo, Fischer, & Krzeminski 1995; Leo II: Siegel & Majewski 2000; Andromeda VI: Paper I; Andromeda II: Paper II). The presence of these stars in the gap indicates that the RRL populations in dSph galaxies are not simply superpositions of two separate populations, one being metal-rich and the other metal-poor. In column 10 of Tables 2 and 3, we list the $\Delta \log P$ values for the RRab stars of And I and And III. These values are plotted against the corresponding $\log P$ values in Figure 12. Clearly, like the other dSph galaxies, both And I and And III have a

substantial number of RRab stars within the gap. This figure also shows the lack of short period RRab stars in And III. The mean period shift is +0.01 for And I and –0.02 for And III. Using $\Delta \log P = 0.116[\text{Fe}/\text{H}] + 0.173$ from Sandage (1982a), we find $[\text{Fe}/\text{H}] = -1.41$ for And I and -1.66 for And III. The value determined for And I is close to that found by DACS00 ($\langle [\text{Fe}/\text{H}] \rangle = -1.46 \pm 0.12$) based on the colors of RGB stars. On the other hand, the estimate for And III is somewhat more metal-rich than that given by DAC02 from the color of the RGB ($\langle [\text{Fe}/\text{H}] \rangle = -1.88 \pm 0.11$). This discrepancy is reduced with the metallicity estimates made in the following section using different methods.

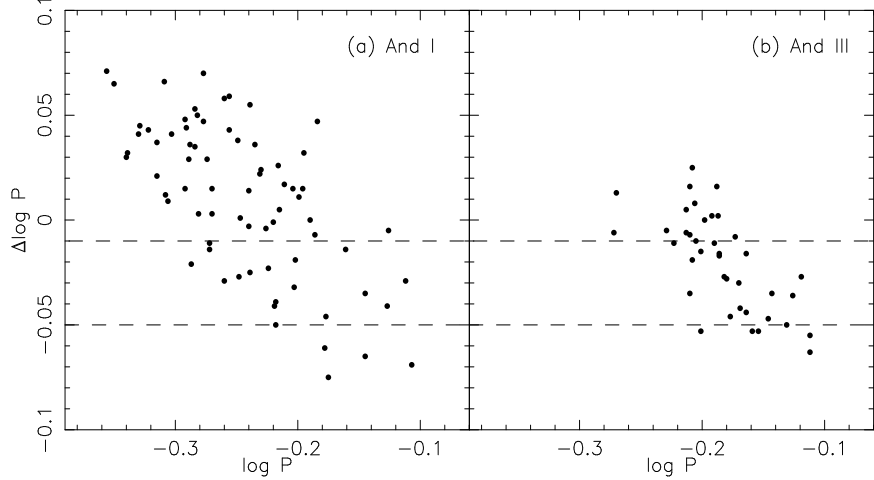


FIG. 12.— Period shift versus period for the RRab stars in (a) And I and (b) And III. The dashed lines represent the zone in which few RRab stars from Galactic globular clusters are found.

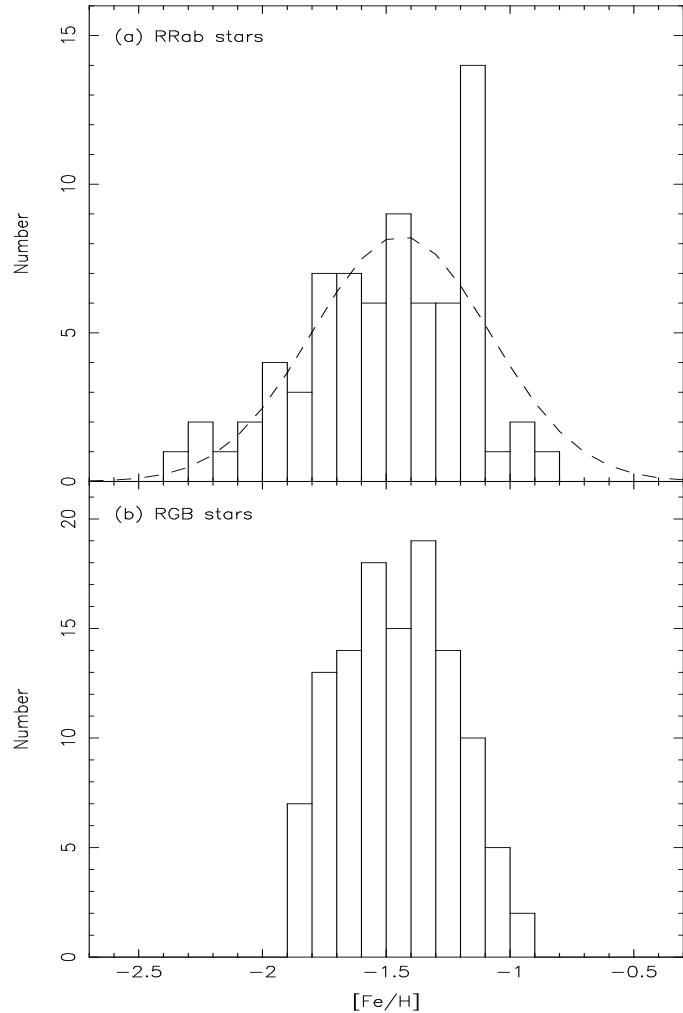


FIG. 13.— Upper panel: [Fe/H] distribution plot for the RRab stars in And I. The individual [Fe/H] values were calculated using Eq. 2 and have an uncertainty of ~ 0.3 dex. The dashed line is a gaussian fit to these data. It has a mean of $[Fe/H] = -1.44$ and a standard deviation of 0.51 dex. Lower panel: [Fe/H] distribution plot for red giant branch stars in And I from DACS00. The individual [Fe/H] values have uncertainties of ~ 0.1 dex.

5.5. Metallicity Estimates from the RR Lyrae Stars

We found in Papers I and II that the equation:

$$[Fe/H]_{ZW} = -8.85(\log P_{ab} + 0.15A_V) - 2.60 \quad (2)$$

derived by Alcock et al. (2000) using the RRab stars in M3, M5, and M15 yields a mean metallicity for the RRL in And II and And VI similar to those found using the mean colors of

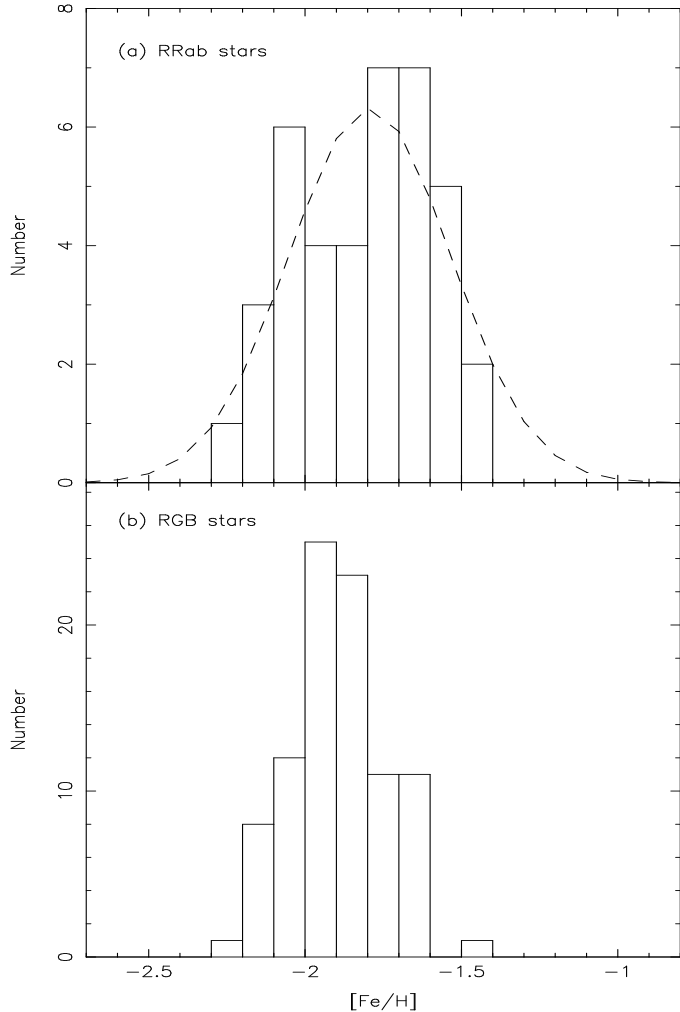


FIG. 14.—Upper panel: [Fe/H] distribution plot for the RRab stars in And III. The individual [Fe/H] values were calculated using Eq. 2 and have an uncertainty of ~ 0.3 dex. The dashed line is a gaussian fit to these data. The curve has a mean of $[Fe/H] = -1.79$ and a standard deviation of 0.37 dex. Lower panel: [Fe/H] distribution plot for red giant branch stars in And III from DAC02. The individual [Fe/H] values have uncertainties of ~ 0.1 dex.

the RGB. The accuracy of this equation is $\sigma_{[Fe/H]} = 0.31$ per star (Alcock et al. 2000). Using this equation, we derived individual metallicities for the RRab stars and these are listed in column 11 in Tables 2 and 3 for And I and And III, respectively.

The upper panel of Figure 13 plots the abundance distribution for the RRab stars in And I using the individual abundances derived from Eq. 2. The mean and median of the values are $[Fe/H] = -1.49$ and -1.46 , respectively. A gaussian fit to these data is also shown which has a mean of $[Fe/H] = -1.44 \pm 0.03$ (standard error of the mean). These RRab based abundances agree well with the mean And I abundance, $[Fe/H] = -1.46 \pm 0.12$, determined by DACS00 from the colors of the red giant branch stars. As noted in Paper II, because not every red giant branch star evolves to become an RRab, there is no obvious reason to expect these mean abundances to agree.

The gaussian fit shown in the upper panel of Fig. 13 has a standard deviation of 0.51 dex. Given that the individual RRL abundances have uncertainties of order 0.3 dex, this suggests the presence of a real abundance dispersion among the And I RRab stars, with $\sigma_{[Fe/H],int} \sim 0.4$ dex. This value is somewhat larger than the abundance dispersion found by DACS00 from

the And I red giant branch ($\sigma_{[Fe/H],int} \sim 0.21$) though, again recognizing that not every red giant branch star evolves to become a RRab star, it is difficult to compare these dispersions in a meaningful way. The lower panel of Fig. 13 shows the red giant branch abundance distribution for And I from DACS00. Given that the individual red giant branch abundance determinations have substantially lower uncertainties than the RRab values, the distributions appear quite comparable. Both distributions appear to be sharply limited on the metal-rich side. The And I results are similar to the situation for And II, where both the RRab and the red giant branch stars show substantial abundance ranges, larger indeed than those found here for And I (Paper II).

For And III, the distribution of the individual metallicity estimates for the RRab stars is shown in the upper panel of Figure 14. Here the mean and median metallicity values are -1.81 and -1.77 , respectively. The gaussian fit to the data has a mean value of -1.79 ± 0.03 (standard error of the mean). Once again, despite the fact that only a relatively small fraction of the red giant branch stars evolve to become RRab stars (cf. Fig. 1), these RRab based abundance values agree well with the red giant branch based determination of the mean abundance, $[Fe/H] = -1.88 \pm 0.11$, given by DAC02.

The gaussian fit shown in Fig. 14 has a standard deviation of 0.37 dex, considerably smaller than was found for And I, and barely larger than that expected on the basis of the individual errors alone (~ 0.3 dex). There is therefore no compelling case for the existence of a substantial abundance spread among the And III RRab stars. This result is similar to that found for the RRab in And VI (Paper I). Again while there is no reason to expect this to be the case, the small abundance dispersion for the And III RRab stars is consistent with the results for the red giant branch: DAC02 give $\sigma_{[\text{Fe}/\text{H}],\text{int}} = 0.12$ from their analysis of the red giant branch colors. The lower panel of Fig. 14 reinforces this conclusion: it shows the red giant branch abundance distribution from DAC02. As for Fig. 13, given the larger uncertainty in the individual RRab values, the distribution in the upper and lower panels appear quite similar.

Now that we have used the Alcock et al. (2000) equation (Eq. 2) to estimate the mean metallicity for the RRL in four of the M31 dSph galaxies, it is worthwhile to evaluate the outcome of this process. Even though the metallicity estimate for any individual RRL from this equation is of limited accuracy, for each of the four dSph galaxies the mean metallicity derived from the RRL stars is in excellent accord with that determined from the RGB. Indeed, for these four systems, the standard deviation of the differences between the RRL and RGB metallicity estimates is only 0.05 dex. Since not every RGB star evolves into an RRL, there is no *a priori* reason to expect this good agreement. Yet clearly the RRL stars, and the use of Eq. 2, are providing valid estimates of the mean metallicities of these four systems. Consequently, application of Eq. 2 may prove worthwhile in those situations where information is available only for RRL stars. Further applications to other dSph galaxies and globular clusters will be important to test the application of this equation.

6. SUMMARY & CONCLUSIONS

We have presented the results of variable star surveys of the M31 dSph galaxies And I and And III using the HST/WFPC2. And I was found to contain 72 fundamental mode and 26 first-overtone mode RRL stars with mean periods of 0.575 day and 0.388 day, respectively, with one unclassified RRL star. We also found that two of the RRL in the And I field are fainter than the HB; these stars may be associated with the recently discovered stellar stream in the halo of M31. In And III, we discovered 39 fundamental mode and 12 first-overtone mode RRL stars with mean periods of 0.657 day and 0.402 day, respectively. The mean period of the RRab stars in And I is consistent with the Galactic globular cluster RRL mean period - metallicity relation. For And III, the mean period of the RRab stars is longer than that expected for the mean metallicity of the galaxy. This discrepancy arises from a lack of shorter period, higher amplitude RRab stars in And III compared to other dSphs. This effect may be related to the very red morphology of the HB in this dSph. We also find for both dSph galaxies that the mean magnitudes of the RRL imply distances similar to those previously determined from the mean magnitude of the horizontal branch.

We found five variable stars that are brighter than the HB in And III, four of which are ACs. These stars have properties consistent with ACs found in other dSph galaxies in terms of their P-L and period-amplitude relations. The other star, and the single supra-HB star in And I, may be P2C variables rather than ACs. Further observations are needed to clarify their nature though we note that in the Galactic globular cluster popu-

lation, P2Cs are found only in those clusters with strong blue HB morphology, which both And I and And III lack. Assuming that these two stars are ACs, we have included the resulting AC specific frequencies for And I and And III with the data for other dSph galaxies from Paper II. These AC specific frequencies follow the trends defined by the other dSphs when plotted against both (visual) luminosity and mean abundance. As we concluded in Paper II, there is a clear correlation between the AC specific frequency and dSph luminosity (and mean abundance) as first noted by Mateo et al. (1995).

For the RRab stars in And I, we found $\langle [\text{Fe}/\text{H}] \rangle = -1.49$ from the Alcock et al. (2000) equation that relates the metallicity of a RRab star to its period and amplitude. This mean abundance estimate agrees well with that of DACS00, $\langle [\text{Fe}/\text{H}] \rangle = -1.46 \pm 0.12$, determined from the colors of the red giant branch stars. For And III, applying the same method yields $\langle [\text{Fe}/\text{H}] \rangle = -1.81$ from the RRab stars, which again agrees well with the mean abundance from the red giant branch, $\langle [\text{Fe}/\text{H}] \rangle = -1.88 \pm 0.11$ (DAC02). Indeed, we have found that the Alcock et al. (2000) equation provides a good estimate for the mean metallicity for all the four systems we have surveyed despite the fact that not all red giant branch stars evolve to become RRL stars. It remains to be seen how well this equation applies to other dwarf galaxies or globular clusters.

In agreement with Baldacci et al. (2003), Marconi et al. (2004), and Gallart et al. (2004), we find that the short-period Cepheids in dwarf galaxies such as Leo A, Sextans A, and IC 1613 do not follow the same P-L relations as found for the ACs. The short-period Cepheids typically have higher luminosities than the ACs at fixed period.

In summary, our search for variable stars in the M31 dSph companions has, up to this point, revealed that their variable star populations are basically indistinguishable from those of their Galactic counterparts. In particular, the properties and specific frequencies of the ACs in the M31 dSph galaxies are similar to those found in the Galactic dSph galaxies. Further, the properties of the RRL stars are consistent with those found in the Galactic dSphs, and have been shown to be good indicators for the distance and, perhaps surprisingly, also the mean metallicity for these M31 dSph companions.

This research was supported in part by NASA through grant number GO-08272 from the Space Telescope Science Institute, which is operated by AURA, Inc., under NASA contract NAS 5-26555.

Thank you to the referee for the valuable comments for this paper. We would like to thank P. B. Stetson for graciously sharing his PSFs for the WFPC2 and for the use of his data reduction programs. Thanks to A. C. Layden for the use of his light curve analysis programs. GDaC is grateful to Andrew Drake for his efforts in carrying out the initial analysis of the variable stars in And I. Thanks also to M. Catelan and H. A. Smith for discussions on the RRL period distribution in And III.

REFERENCES

Alcock, C., et al. 2000, AJ, 119, 2194

Armandroff, T. E., Davies, J. E., & Jacoby, G. H. 1998, AJ, 116, 2287

Armandroff, T. E., Jacoby, G. H., & Davies, J. E. 1999, AJ, 118, 1220

Baldacci, L., Clementini, G., Held, E. V., Marconi, M., & Rizzi, L. 2003, in Communications in Asteroseismology, in press (astro-ph/0311170)

Bersier, D., & Wood, P. R. 2002, AJ, 123, 840

Bono, G., Caputo, F., Santolamazza, P., Cassisi, S., & Piersimoni, A. 1997, AJ, 113, 2209

Brown, T. M., Ferguson, H. C., Smith, E., Kimble, R. A., Sweigart, A. V., Renzini, A., Rich, R. M., & VandenBerg, D. A. 2003, ApJ, 592, L17

Brown, T. M., Ferguson, H. C., Smith, E., Kimble, R. A., Sweigart, A. V., Renzini, A., & Rich, R. M. 2004, AJ, 127, 2738

Caldwell, N., Armandroff, T. E., Seitzer, P., & Da Costa, G. S. 1992, AJ, 103, 840

Catelan, M. 2004, in IAU Colloq. 193, Variable Stars in the Local Group, ed. D. W. Kurtz & K. R. Pollard (San Francisco: ASP), 113

Clementini, G., Held, E. V., Baldacci, L., & Rizzi, L. 2003, ApJ, 588, L85

Da Costa, G. S., Armandroff, T. E., & Caldwell, N. 2002, AJ, 124, 332 (DAC02)

Da Costa, G. S., Armandroff, T. E., Caldwell, N., & Seitzer, P. 1996, AJ, 112, 2576 (DACS96)

Da Costa, G. S., Armandroff, T. E., Caldwell, N., & Seitzer, P. 2000, AJ, 119, 705 (DACS00)

Da Costa, G. S., Drake, A., Armandroff, T. E., & Caldwell, N. 1997, in Dwarf Galaxies: Probes for Galaxy Formation and Evolution

Demarque, P., & Hirshfeld, A. W. 1975, ApJ, 202, 346

Dolphin, A. E., et al. 2001, ApJ, 550, 554

Dolphin, A. E., et al. 2002, AJ, 123, 3154

Dolphin, A. E., et al. 2003, AJ, 125, 1261

Durrell, P. R., Harris, W. E., & Pritchett, C. J. 2004, AJ, 128, 260

Ferguson, A. M. N., Irwin, M. J., Ibata, R. A., Lewis, G. F., & Tanvir, N. R. 2002, AJ, 124, 1452

Gallart, C., Aparicio, A., Freedman, W. L., Madore, B. F., Martínez-Delgado, D., & Stetson, P. B. 2004, AJ, 127, 1486

Ibata, R., Irwin, M., Lewis, G., Ferguson, A. M. N., & Tanvir, N. 2001, Nature, 412, 49

Karachentsev, I. D., & Karachentseva, V. E. 1999, A&A, 341, 355

Lee, Y. W., Demarque, P., & Zinn, R. 1990, ApJ, 350, 155

Marconi, M., Fiorentino, G., & Caputo, F. 2004, A&A, 417, 1101

Mateo, M., Fischer, P., & Krzeminski, W. 1995, AJ, 110, 2166

McConnachie, A. W., Irwin, M. J., Ibata, R. A., Ferguson, A. M. N., Lewis, G. F., & Tanvir, N. 2003, MNRAS, 343, 1335

McNamara, D. H. 1995, AJ, 109, 2134

Nemec, J. M., Nemec, A. F. L., & Lutz, T. E. 1994, AJ, 108, 222

Olszewski, E. W., & Aaronson, M. 1985, AJ, 90, 2221

Pritchett, C. J., & van den Bergh, S. 1994, AJ, 107, 1730

Pritzl, B. J., Armandroff, T. E., Jacoby, G. H., & Da Costa, G. S. 2002, AJ, 124, 1464 (Paper I)

Pritzl, B. J., Armandroff, T. E., Jacoby, G. H., & Da Costa, G. S. 2004, AJ, 127, 318 (Paper II)

Sandage, A. 1981, ApJ, 248, 161

Sandage, A. 1982a, ApJ, 252, 553

Sandage, A. 1982b, ApJ, 252, 574

Sandage, A., Katem, B., & Sandage, M. 1981, ApJS, 46, 41

Saviane, I., Held, E. V., & Bertelli, G. 2000, A&A, 355, 56

Siegel, M. H., & Majewski, S. R. 2000, AJ, 120, 284

Stetson, P. B. 1994, PASP, 106, 250

Wallerstein, G. 2002, PASP, 114, 689

TABLE 1
PHOTOMETRIC DIFFERENCES

| | Chip | V | B |
|----------|------|-------|-------|
| And I: | WFC2 | -0.07 | -0.10 |
| | WFC3 | -0.05 | -0.09 |
| | WFC4 | -0.07 | -0.08 |
| | PC | -0.05 | -0.08 |
| | WFC2 | -0.02 | -0.05 |
| | WFC3 | -0.03 | -0.05 |
| And III: | WFC4 | -0.01 | -0.03 |

NOTE. — difference = magnitude
in present study - CMD magnitude

TABLE 2
LIGHT CURVE PROPERTIES FOR AND I

| ID | RA (2000) | Dec (2000) | Period | $\langle V \rangle$ | $\langle B \rangle$ | $(B-V)_{\text{mag}}$ | A_V | A_B | $\Delta \log P$ | [Fe/H] | Classification |
|-----|------------|------------|--------|---------------------|---------------------|----------------------|-------|-------|-----------------|--------|--------------------|
| V01 | 0:45:42.18 | 38:02:51.8 | 1.630 | 24.336 | 24.665 | 0.338 | 0.39 | 0.55 | ... | ... | AC?, P2C? |
| V02 | 0:45:42.59 | 38:02:43.9 | 0.348 | 24.802 | 25.153 | 0.366 | 0.50 | 0.71 | ... | ... | c |
| V03 | 0:45:42.57 | 38:03:00.4 | 0.412 | 25.084 | 25.404 | 0.334 | 0.48 | 0.68 | ... | ... | c; Drake: P=0.383 |
| V04 | 0:45:42.16 | 38:02:47.0 | ... | ... | ... | ... | ... | ... | ... | ... | RRL?; No F555W |
| V05 | 0:45:41.10 | 38:03:03.9 | 0.654 | 25.053 | 25.522 | 0.473 | 0.27 | 0.39 | 0.05 | -1.33 | ab |
| V06 | 0:45:42.63 | 38:03:14.1 | 0.430 | 25.010 | 24.434 | 0.433 | 0.38 | 0.54 | ... | ... | c |
| V07 | 0:45:40.30 | 38:03:47.2 | 0.338 | 25.137 | 25.528 | 0.408 | 0.55 | 0.77 | ... | ... | c; Drake: P=0.358 |
| V08 | 0:45:39:27 | 38:03:33.0 | 0.376 | 25.019 | 25.502 | 0.493 | 0.43 | 0.61 | ... | ... | c |
| V09 | 0:45:43.68 | 38:03:49.0 | 0.413 | 25.139 | 25.567 | 0.447 | 0.57 | 0.81 | ... | ... | c |
| V10 | 0:45:44.89 | 38:03:24.7 | 0.664 | 25.048 | 25.442 | 0.423 | 0.83 | 1.17 | -0.06 | -2.13 | ab; Drake: P=0.667 |
| V11 | 0:45:41.64 | 38:03:18.0 | 0.349 | 25.226 | 25.568 | 0.349 | 0.35 | 0.49 | ... | ... | c |
| V12 | 0:45:42.17 | 38:03:47.3 | 0.367 | 25.145 | 25.436 | 0.303 | 0.46 | 0.65 | ... | ... | c; Drake: P=0.323 |
| V13 | 0:45:42.30 | 38:02:59.6 | 0.716 | 25.082 | 25.459 | 0.395 | 0.67 | 0.95 | -0.07 | -2.21 | ab |
| V14 | 0:45:38.82 | 38:03:08.0 | 0.471 | 25.145 | 25.533 | 0.394 | 0.31 | 0.44 | ... | ... | c; Drake: P=0.367 |
| V15 | 0:45:40.89 | 38:03:00.2 | 0.355 | 25.187 | 25.561 | 0.383 | 0.42 | 0.59 | ... | ... | c; Drake: P=0.355 |
| V16 | 0:45:43.53 | 38:03:32.9 | 0.665 | 25.061 | 25.510 | 0.472 | 0.74 | 1.05 | -0.05 | -2.02 | ab |
| V17 | 0:45:43.32 | 38:02:53.6 | 0.350 | 25.265 | 25.663 | 0.404 | 0.39 | 0.56 | ... | ... | c |
| V18 | 0:45:40.20 | 38:03:23.0 | 0.529 | 25.126 | 25.600 | 0.500 | 0.78 | 1.10 | 0.05 | -1.19 | ab; Drake: P=0.479 |
| V19 | 0:45:42.91 | 38:03:39.3 | 0.458 | 25.218 | 25.432 | 0.278 | 1.19 | 1.70 | 0.03 | -1.18 | ab |
| V20 | 0:45:41.04 | 38:03:58.0 | 0.513 | 25.254 | 25.583 | 0.337 | 0.42 | 0.60 | ... | ... | c; Drake: P=0.509 |
| V21 | 0:45:43.64 | 38:03:26.7 | 0.470 | 25.323 | 25.703 | 0.385 | 0.29 | 0.41 | ... | ... | c |
| V22 | 0:45:43.70 | 38:03:04.4 | 0.484 | 25.173 | 25.538 | 0.420 | 1.13 | 1.60 | 0.02 | -1.31 | ab |
| V23 | 0:45:41.91 | 38:03:31.0 | 0.471 | 25.358 | 25.692 | 0.340 | 0.37 | 0.52 | ... | ... | c |
| V24 | 0:45:42.91 | 38:02:38.5 | 0.491 | 25.052 | 25.504 | 0.484 | 0.85 | 1.20 | 0.07 | -1.00 | ab; Drake: P=0.491 |
| V25 | 0:45:40.91 | 38:03:25.0 | 0.615 | 25.206 | 25.661 | 0.471 | 0.58 | 0.82 | 0.02 | -1.50 | ab |
| V26 | 0:45:43.83 | 38:03:24.4 | 0.515 | 25.157 | 25.598 | 0.477 | 0.90 | 1.27 | 0.04 | -1.25 | ab |
| V27 | 0:45:42.96 | 38:03:19.3 | 0.577 | 25.081 | 25.515 | 0.473 | 0.97 | 1.36 | -0.03 | -1.77 | ab |
| V28 | 0:45:41.56 | 38:03:09.4 | 0.510 | 25.089 | 25.517 | 0.474 | 1.04 | 1.47 | 0.02 | -1.39 | ab; Drake: P=0.567 |
| V29 | 0:45:40.02 | 38:03:07.7 | 0.498 | 25.173 | 25.530 | 0.401 | 0.95 | 1.35 | 0.04 | -1.18 | ab |
| V30 | 0:45:42.55 | 38:03:28.7 | 0.381 | 25.212 | 25.642 | 0.450 | 0.60 | 0.80 | ... | ... | c |
| V31 | 0:45:45.14 | 38:03:22.6 | 0.494 | 25.032 | 25.408 | 0.433 | 1.15 | 1.62 | 0.01 | -1.41 | ab |
| V32 | 0:45:42.84 | 38:03:28.4 | 0.582 | 25.196 | 25.663 | 0.482 | 0.61 | 0.86 | 0.04 | -1.33 | ab |
| V33 | 0:45:42.73 | 38:03:23.1 | 0.537 | 25.220 | 25.652 | 0.473 | 0.92 | 1.29 | 0.02 | -1.42 | ab; Drake: P=0.537 |
| V34 | 0:45:42.64 | 38:02:55.6 | 0.510 | 25.224 | 25.596 | 0.405 | 0.86 | 1.22 | 0.05 | -1.15 | ab |
| V35 | 0:45:38.84 | 38:02:59.0 | 0.637 | 25.359 | 25.755 | 0.408 | 0.51 | 0.72 | 0.02 | -1.54 | ab |
| V36 | 0:45:41.32 | 38:03:15.9 | 0.575 | 25.180 | 25.629 | 0.476 | 0.76 | 1.07 | 0.01 | -1.48 | ab |
| V37 | 0:45:42.75 | 38:02:42.3 | 0.534 | 25.184 | 25.568 | 0.434 | 1.09 | 1.54 | -0.01 | -1.63 | ab; Drake: P=0.674 |
| V38 | 0:45:42.49 | 38:03:34.9 | 0.520 | 25.199 | 25.648 | 0.480 | 0.79 | 1.11 | 0.05 | -1.13 | ab |
| V39 | 0:45:38.45 | 38:03:18.2 | 0.517 | 25.161 | 25.578 | 0.480 | 1.21 | 1.70 | -0.02 | -1.66 | ab; Drake: P=0.569 |
| V40 | 0:45:41.62 | 38:03:17.8 | 0.522 | 25.231 | 25.676 | 0.474 | 0.79 | 1.12 | 0.05 | -1.15 | ab |
| V41 | 0:45:41.47 | 38:02:57.4 | 0.484 | 25.254 | 25.616 | 0.419 | 1.05 | 1.48 | 0.04 | -1.20 | ab; Drake: P=0.591 |
| V42 | 0:45:40.04 | 38:03:29.4 | 0.447 | 25.282 | 25.686 | 0.465 | 1.08 | 1.53 | 0.07 | -0.94 | ab |
| V43 | 0:45:39.62 | 38:03:42.3 | 0.746 | 25.276 | 25.650 | 0.383 | 0.44 | 0.62 | -0.04 | -2.06 | ab |
| V44 | 0:45:43.99 | 38:03:10.9 | 0.748 | 25.169 | 25.552 | 0.386 | 0.24 | 0.33 | -0.01 | -1.80 | ab |
| V45 | 0:45:49.15 | 38:02:02.4 | 0.772 | 24.988 | 25.493 | 0.508 | 0.29 | 0.41 | -0.03 | -1.99 | ab |
| V46 | 0:45:45.02 | 38:02:55.0 | 0.589 | 25.039 | 25.456 | 0.438 | 0.64 | 0.91 | 0.02 | -1.42 | ab |
| V47 | 0:45:47.03 | 38:03:14.7 | 0.400 | 25.043 | 25.411 | 0.377 | 0.39 | 0.55 | ... | ... | c; Drake: P=0.399 |
| V48 | 0:45:46.91 | 38:03:27.6 | 0.415 | 25.100 | 25.533 | 0.447 | 0.57 | 0.81 | ... | ... | c |
| V49 | 0:45:47.84 | 38:02:26.7 | 0.566 | 25.200 | 25.651 | 0.488 | 0.88 | 1.23 | 0.00 | -1.58 | ab; Drake: P=0.513 |
| V50 | 0:45:45.73 | 38:02:27.4 | 0.389 | 25.067 | 25.503 | 0.440 | 0.27 | 0.38 | ... | ... | c; Drake: P=0.335 |
| V51 | 0:45:48.87 | 38:02:37.8 | 0.363 | 25.118 | 25.652 | 0.546 | 0.44 | 0.62 | ... | ... | c; Drake: P=0.39 |
| V52 | 0:45:47.13 | 38:02:16.1 | 0.646 | 25.146 | 25.639 | 0.507 | 0.56 | 0.79 | 0.00 | -1.66 | ab; Drake: P=0.519 |
| V53 | 0:45:46.67 | 38:02:34.3 | 0.285 | 25.270 | 25.616 | 0.358 | 0.53 | 0.75 | ... | ... | c; Drake: P=0.522 |
| V54 | 0:45:50.71 | 38:02:42.8 | 0.597 | 24.932 | 25.330 | 0.436 | 0.87 | 1.23 | -0.02 | -1.77 | ab |
| V55 | 0:45:44.30 | 38:02:31.1 | 0.606 | 24.969 | 25.309 | 0.381 | 0.98 | 1.39 | -0.05 | -1.98 | ab |

TABLE 2
LIGHT CURVE PROPERTIES FOR AND I

| | | | | | | | | | | | |
|------|------------|------------|-------|--------|--------|-------|------|------|-------|-------|--------------------|
| V56 | 0:45:46.20 | 38:03:17.5 | 0.628 | 25.119 | 25.602 | 0.508 | 0.73 | 1.03 | -0.02 | -1.78 | ab |
| V57 | 0:45:48.17 | 38:02:07.0 | 0.587 | 25.117 | 25.550 | 0.452 | 0.67 | 0.94 | 0.02 | -1.44 | ab; Drake: P=0.585 |
| V58 | 0:45:47.87 | 38:02:40.4 | 0.532 | 25.182 | 25.591 | 0.447 | 0.86 | 1.22 | 0.03 | -1.32 | ab; Drake: P=0.533 |
| V59 | 0:45:47.06 | 38:02:18.5 | 0.492 | 25.246 | 25.570 | 0.380 | 1.14 | 1.61 | 0.01 | -1.39 | ab; Drake: P=0.541 |
| V60 | 0:45:46.49 | 38:02:16.6 | 0.626 | 24.964 | 25.420 | 0.485 | 0.81 | 1.14 | -0.03 | -1.87 | ab |
| V61 | 0:45:45.37 | 38:02:27.7 | 0.554 | 25.192 | 25.651 | 0.474 | 0.60 | 0.85 | 0.06 | -1.13 | ab |
| V62 | 0:45:44.91 | 38:02:25.5 | 0.691 | 25.237 | 25.741 | 0.515 | 0.48 | 0.67 | -0.01 | -1.82 | ab; Drake: P=0.618 |
| V63 | 0:45:47.95 | 38:02:40.8 | 0.456 | 25.251 | 25.734 | 0.490 | 0.35 | 0.49 | ... | ... | c; Drake: P=0.388 |
| V64 | 0:45:45.35 | 38:02:30.6 | 0.564 | 25.178 | 25.649 | 0.490 | 0.67 | 0.95 | 0.04 | -1.29 | ab |
| V65 | 0:45:48.55 | 38:02:20.1 | 0.549 | 25.147 | 25.585 | 0.490 | 1.11 | 1.56 | -0.03 | -1.77 | ab; Drake: P=0.499 |
| V66 | 0:45:46.07 | 38:03:11.0 | 0.514 | 25.183 | 25.617 | 0.479 | 0.95 | 1.33 | 0.03 | -1.30 | ab; Drake: P=0.513 |
| V67 | 0:45:43.99 | 38:02:25.2 | 0.363 | 25.346 | 25.745 | 0.406 | 0.35 | 0.50 | ... | ... | c |
| V68 | 0:45:45.44 | 38:02:30.4 | 0.555 | 25.222 | 25.657 | 0.456 | 0.69 | 0.97 | 0.04 | -1.25 | ab; Drake: P=0.496 |
| V69 | 0:45:48.95 | 38:03:15.0 | 0.512 | 25.175 | 25.591 | 0.448 | 0.87 | 1.23 | 0.04 | -1.18 | ab; Drake: P=0.514 |
| V70 | 0:45:45.84 | 38:02:34.0 | 0.608 | 25.205 | 25.703 | 0.512 | 0.56 | 0.79 | 0.03 | -1.43 | ab |
| V71 | 0:45:49.91 | 38:02:41.0 | 0.576 | 25.119 | 25.525 | 0.437 | 0.85 | 1.20 | 0.00 | -1.61 | ab |
| V72 | 0:45:44.42 | 38:02:42.9 | 0.441 | 25.135 | 25.517 | 0.440 | 1.08 | 1.52 | 0.07 | -0.89 | ab |
| V73 | 0:45:45.65 | 38:02:39.8 | 0.537 | 25.223 | 25.647 | 0.471 | 0.99 | 1.39 | 0.00 | -1.52 | ab |
| V74 | 0:45:49.21 | 38:02:30.9 | 0.535 | 25.248 | 25.568 | 0.380 | 1.07 | 1.51 | -0.01 | -1.62 | ab |
| V75 | 0:45:47.46 | 38:02:33.9 | 0.604 | 25.187 | 25.551 | 0.409 | 0.94 | 1.33 | -0.04 | -1.91 | ab; Drake: P=0.599 |
| V76 | 0:45:46.80 | 38:02:31.6 | 0.468 | 25.542 | 25.908 | 0.426 | 1.11 | 1.56 | 0.04 | -1.16 | ab |
| V77 | 0:45:47.50 | 38:03:01.1 | 0.310 | 25.240 | 25.626 | 0.392 | 0.31 | 0.43 | ... | ... | c; Drake: P=0.310 |
| V78 | 0:45:49.64 | 38:02:24.4 | 0.638 | 25.190 | 25.720 | 0.537 | 0.41 | 0.58 | 0.03 | -1.42 | ab; Drake: P=0.645 |
| V79 | 0:45:46.31 | 38:01:51.9 | 0.652 | 24.958 | 25.341 | 0.399 | 0.57 | 0.81 | -0.01 | -1.71 | ab |
| V80 | 0:45:41.50 | 38:01:34.0 | 0.356 | 24.999 | 25.441 | 0.456 | 0.50 | 0.71 | ... | ... | c; Drake: P=0.357 |
| V81 | 0:45:44.16 | 38:01:36.9 | 0.381 | 25.221 | 25.552 | 0.340 | 0.40 | 0.56 | ... | ... | c |
| V82 | 0:45:47.36 | 38:01:25.4 | 0.577 | 25.136 | 25.528 | 0.406 | 0.53 | 0.74 | 0.06 | -1.19 | ab; Drake: P=0.524 |
| V83 | 0:45:45.42 | 38:01:44.0 | 0.529 | 25.246 | 25.643 | 0.416 | 0.65 | 0.92 | 0.07 | -1.02 | ab; Drake: P=0.532 |
| V84 | 0:45:42.40 | 38:02:04.6 | 0.334 | 25.159 | 25.570 | 0.419 | 0.37 | 0.52 | ... | ... | c |
| V85 | 0:45:44.38 | 38:01:18.0 | 0.632 | 25.222 | 25.621 | 0.411 | 0.55 | 0.78 | 0.01 | -1.57 | ab; Drake: P=0.707 |
| V86 | 0:45:44.02 | 38:01:03.6 | 0.549 | 25.144 | 25.651 | 0.527 | 0.64 | 0.89 | 0.06 | -1.14 | ab |
| V87 | 0:45:42.42 | 38:01:22.3 | 0.669 | 25.085 | 25.491 | 0.439 | 0.88 | 1.25 | -0.08 | -2.22 | ab |
| V88 | 0:45:43.01 | 38:02:17.0 | 0.565 | 24.996 | 25.402 | 0.452 | 1.03 | 1.45 | -0.03 | -1.77 | ab |
| V89 | 0:45:44.90 | 38:02:09.8 | 0.523 | 25.180 | 25.467 | 0.335 | 1.05 | 1.48 | 0.00 | -1.50 | ab |
| V90 | 0:45:41.86 | 38:01:36.3 | 0.610 | 25.098 | 25.526 | 0.448 | 0.67 | 0.94 | 0.01 | -1.59 | ab |
| V91 | 0:45:42.03 | 38:01:10.3 | 0.594 | 25.125 | 25.549 | 0.453 | 0.78 | 1.10 | 0.00 | -1.63 | ab |
| V92 | 0:45:43.13 | 38:01:24.0 | 0.469 | 25.062 | 25.381 | 0.379 | 1.07 | 1.52 | 0.05 | -1.11 | ab; Drake: P=0.513 |
| V93 | 0:45:45.42 | 38:00:55.1 | 0.476 | 25.213 | 25.510 | 0.351 | 1.04 | 1.48 | 0.04 | -1.13 | ab |
| V94 | 0:45:42.29 | 38:02:00.6 | 0.605 | 25.258 | 25.747 | 0.530 | 0.93 | 1.31 | -0.04 | -1.90 | ab |
| V95 | 0:45:46.05 | 38:01:16.2 | 0.457 | 25.158 | 25.536 | 0.443 | 1.22 | 1.72 | 0.03 | -1.21 | ab; Drake: P=0.499 |
| V96 | 0:45:46.20 | 38:01:00.1 | 0.520 | 25.271 | 25.711 | 0.479 | 0.89 | 1.25 | 0.04 | -1.27 | ab; Drake: P=0.578 |
| V97 | 0:45:43.30 | 38:01:58.8 | 0.603 | 25.136 | 25.602 | 0.488 | 0.73 | 1.03 | 0.00 | -1.62 | ab |
| V98 | 0:45:46.39 | 38:02:01.9 | 0.625 | 25.209 | 25.586 | 0.393 | 0.55 | 0.78 | 0.02 | -1.52 | ab |
| V99 | 0:45:45.62 | 38:01:13.5 | 0.716 | 25.215 | 25.670 | 0.468 | 0.51 | 0.71 | -0.04 | -1.99 | ab |
| V100 | 0:45:42.36 | 38:02:00.5 | 0.782 | 25.766 | 26.208 | 0.453 | 0.49 | 0.68 | -0.07 | -2.31 | ab |

NOTE. — The periods referenced as Drake derive from the first year Ph.D. project (1996) of A. Drake with supervisor G. S. Da Costa. The published reference to this data is Da Costa et al. (1997).

TABLE 3
 LIGHT CURVE PROPERTIES FOR AND III

| ID | RA (2000) | Dec (2000) | Period | $\langle V \rangle$ | $\langle B \rangle$ | $(B-V)_{\text{mag}}$ | A_V | A_B | $\Delta \log P$ | [Fe/H] | Classification |
|-----|------------|------------|--------|---------------------|---------------------|----------------------|-------|-------|-----------------|--------|----------------|
| V01 | 0:35:32.06 | 36:30:38.2 | 0.834 | 23.517 | 23.723 | 0.285 | 1.88 | 1.33 | ... | ... | AC |
| V02 | 0:35:31.74 | 36:30:23.8 | 0.590 | 25.013 | 25.287 | 0.307 | 0.80 | 1.13 | -0.01 | -1.63 | ab |
| V03 | 0:35:30.63 | 36:30:37.2 | 0.773 | 25.033 | 25.367 | 0.349 | 0.47 | 0.67 | -0.06 | -2.23 | ab |
| V04 | 0:35:31.22 | 36:30:21.1 | 0.629 | 25.031 | 25.308 | 0.313 | 0.91 | 1.29 | -0.05 | -2.03 | ab |
| V05 | 0:35:31.42 | 36:30:37.5 | 0.650 | 25.024 | 25.350 | 0.342 | 0.53 | 0.75 | 0.00 | -1.65 | ab |
| V06 | 0:35:36.28 | 36:29:30.4 | 0.678 | 23.166 | 23.575 | 0.433 | 0.93 | 0.66 | ... | ... | AC |
| V07 | 0:35:32.61 | 36:29:05.1 | 0.480 | 23.999 | 24.458 | 0.476 | 0.83 | 0.59 | ... | ... | AC |
| V08 | 0:35:33.01 | 36:29:14.7 | 1.51 | 24.303 | 24.821 | 0.534 | 0.89 | 0.63 | ... | ... | AC?, P2C? |
| V09 | 0:35:35.88 | 36:29:28.6 | 0.501 | 24.584 | 24.993 | 0.436 | 1.14 | 0.81 | ... | ... | AC |
| V10 | 0:35:32.51 | 36:30:05.0 | 0.678 | 25.037 | 25.322 | 0.305 | 0.67 | 0.95 | -0.04 | -2.00 | ab |
| V11 | 0:35:32.27 | 36:30:15.3 | 0.302 | 24.891 | 25.256 | 0.378 | 0.46 | 0.65 | ... | ... | c |
| V12 | 0:35:33.58 | 36:30:04.7 | 0.434 | 24.853 | 25.332 | 0.489 | 0.47 | 0.67 | ... | ... | c |
| V13 | 0:35:31.67 | 36:29:31.3 | 0.652 | 24.947 | 25.333 | 0.402 | 0.63 | 0.89 | -0.02 | -1.79 | ab |
| V14 | 0:35:34.29 | 36:29:17.1 | 0.666 | 25.093 | 25.328 | 0.442 | 0.74 | 1.04 | -0.05 | -2.02 | ab |
| V15 | 0:35:32.77 | 36:29:58.2 | 0.630 | 24.942 | 25.328 | 0.410 | 0.70 | 0.99 | -0.02 | -1.75 | ab |
| V16 | 0:35:34.93 | 36:29:43.9 | 0.620 | 25.054 | 25.295 | 0.266 | 0.76 | 1.08 | -0.02 | -1.77 | ab |
| V17 | 0:35:32.84 | 36:29:42.7 | 0.686 | 25.072 | 25.514 | 0.461 | 0.66 | 0.93 | -0.04 | -2.02 | ab |
| V18 | 0:35:36.01 | 36:29:25.4 | 0.613 | 24.972 | 25.293 | 0.345 | 0.66 | 0.93 | 0.01 | -1.59 | ab |
| V19 | 0:35:35.74 | 36:29:56.3 | 0.646 | 25.048 | 25.374 | 0.356 | 0.62 | 0.87 | -0.01 | -1.74 | ab |
| V20 | 0:35:31.16 | 36:29:04.1 | 0.661 | 24.977 | 25.425 | 0.468 | 0.66 | 0.93 | -0.03 | -1.88 | ab |
| V21 | 0:35:33.16 | 36:29:33.9 | 0.772 | 25.125 | 25.506 | 0.391 | 0.44 | 0.62 | -0.06 | -2.18 | ab |
| V22 | 0:35:36.68 | 36:29:09.9 | 0.455 | 24.968 | 25.352 | 0.407 | 0.68 | 0.96 | ... | ... | c |
| V23 | 0:35:32.94 | 36:29:59.1 | 0.616 | 25.003 | 25.343 | 0.355 | 0.58 | 0.83 | 0.02 | -1.51 | ab |
| V24 | 0:35:33.34 | 36:29:55.3 | 0.624 | 25.022 | 25.487 | 0.488 | 0.70 | 0.98 | -0.01 | -1.71 | ab |
| V25 | 0:35:27.61 | 36:29:45.6 | 0.761 | 24.892 | 25.351 | 0.464 | 0.32 | 0.44 | -0.03 | -1.97 | ab |
| V26 | 0:35:26.38 | 36:29:52.8 | 0.652 | 24.920 | 25.314 | 0.409 | 0.58 | 0.81 | -0.02 | -1.72 | ab |
| V27 | 0:35:26.61 | 36:29:59.5 | 0.491 | 25.091 | 25.443 | 0.365 | 0.48 | 0.67 | ... | ... | c |
| V28 | 0:35:29.88 | 36:29:33.9 | 0.702 | 25.069 | 25.495 | 0.447 | 0.66 | 0.92 | -0.05 | -2.11 | ab |
| V29 | 0:35:30.35 | 36:29:48.0 | 0.648 | 25.089 | 25.433 | 0.354 | 0.46 | 0.65 | 0.02 | -1.54 | ab |
| V30 | 0:35:30.42 | 36:29:47.0 | 0.740 | 25.117 | 25.431 | 0.326 | 0.51 | 0.72 | -0.05 | -2.11 | ab |
| V31 | 0:35:27.56 | 36:29:07.3 | 0.634 | 24.989 | 25.391 | 0.418 | 0.60 | 0.85 | 0.00 | -1.65 | ab |
| V32 | 0:35:28.94 | 36:29:20.0 | 0.617 | 25.070 | 25.388 | 0.349 | 0.86 | 1.22 | -0.04 | -1.88 | ab |
| V33 | 0:35:30.41 | 36:29:47.5 | 0.686 | 25.054 | 25.418 | 0.376 | 0.50 | 0.71 | -0.02 | -1.82 | ab |
| V34 | 0:35:30.70 | 36:30:12.3 | 0.617 | 25.039 | 25.350 | 0.332 | 0.71 | 1.00 | -0.01 | -1.68 | ab |
| V35 | 0:35:27.17 | 36:30:15.1 | 0.283 | 25.080 | 25.569 | 0.504 | 0.58 | 0.81 | ... | ... | c |
| V36 | 0:35:25.85 | 36:29:30.5 | 0.440 | 25.079 | 25.336 | 0.294 | 0.79 | 1.12 | ... | ... | c |
| V37 | 0:35:28.67 | 36:29:29.7 | 0.676 | 24.958 | 25.366 | 0.426 | 0.62 | 0.87 | -0.03 | -1.91 | ab |
| V38 | 0:35:30.11 | 36:31:12.1 | 0.714 | 24.932 | 25.265 | 0.348 | 0.58 | 0.82 | -0.05 | -2.07 | ab |
| V39 | 0:35:24.52 | 36:31:06.8 | 0.620 | 24.789 | 25.138 | 0.361 | 0.52 | 0.74 | 0.03 | -1.45 | ab |
| V40 | 0:35:27.07 | 36:30:45.9 | 0.407 | 24.933 | 25.253 | 0.339 | 0.57 | 0.81 | ... | ... | c |
| V41 | 0:35:28.70 | 36:30:17.4 | 0.671 | 24.983 | 25.386 | 0.415 | 0.51 | 0.72 | -0.01 | -1.74 | ab |
| V42 | 0:35:27.32 | 36:30:37.7 | 0.643 | 24.974 | 25.346 | 0.388 | 0.56 | 0.79 | 0.00 | -1.64 | ab |
| V43 | 0:35:29.74 | 36:30:36.0 | 0.362 | 25.088 | 25.397 | 0.323 | 0.48 | 0.68 | ... | ... | c |
| V44 | 0:35:27.70 | 36:31:02.4 | 0.537 | 24.914 | 25.265 | 0.394 | 0.93 | 1.31 | 0.01 | -1.44 | ab |
| V45 | 0:35:30.16 | 36:30:54.7 | 0.749 | 25.059 | 25.432 | 0.380 | 0.40 | 0.57 | -0.04 | -2.03 | ab |
| V46 | 0:35:29.22 | 36:30:27.6 | 0.353 | 25.061 | 25.351 | 0.308 | 0.56 | 0.79 | ... | ... | c |
| V47 | 0:35:29.09 | 36:30:32.7 | 0.657 | 25.037 | 25.372 | 0.353 | 0.67 | 0.94 | -0.03 | -1.87 | ab |
| V48 | 0:35:26.84 | 36:30:39.3 | 0.613 | 24.951 | 25.378 | 0.452 | 0.72 | 1.01 | -0.01 | -1.67 | ab |
| V49 | 0:35:28.16 | 36:30:15.2 | 0.720 | 25.010 | 25.432 | 0.434 | 0.49 | 0.70 | -0.04 | -1.99 | ab |
| V50 | 0:35:26.92 | 36:30:19.0 | 0.354 | 25.154 | 25.444 | 0.312 | 0.61 | 0.86 | ... | ... | c |
| V51 | 0:35:25.06 | 36:30:17.7 | 0.693 | 24.983 | 25.278 | 0.314 | 0.68 | 0.96 | -0.05 | -2.09 | ab |
| V52 | 0:35:27.25 | 36:30:17.2 | 0.447 | 25.116 | 25.407 | 0.301 | 0.42 | 0.59 | ... | ... | c |
| V53 | 0:35:29.07 | 36:30:22.1 | 0.534 | 25.085 | 25.387 | 0.356 | 1.04 | 1.48 | -0.01 | -1.57 | ab |
| V54 | 0:35:29.14 | 36:30:36.6 | 0.623 | 25.081 | 25.423 | 0.360 | 0.60 | 0.85 | 0.01 | -1.58 | ab |
| V55 | 0:35:28.25 | 36:30:49.1 | 0.599 | 25.013 | 25.294 | 0.308 | 0.80 | 1.13 | -0.01 | -1.69 | ab |
| V56 | 0:35:29.44 | 36:31:22.3 | 0.496 | 24.924 | 25.249 | 0.339 | 0.53 | 0.75 | ... | ... | c |

TABLE 4
B PHOTOMETRY OF THE VARIABLE STARS IN AND I

| HJD-2449000 | V01 | | V02 | |
|-------------|----------|------------|----------|------------|
| | <i>B</i> | σ_B | <i>B</i> | σ_B |
| 575.837 | 24.937 | 0.089 | 24.833 | 0.064 |
| 575.904 | 24.779 | 0.108 | 24.923 | 0.055 |
| 575.971 | 24.896 | 0.118 | 25.279 | 0.096 |
| 576.038 | 24.920 | 0.140 | 25.456 | 0.086 |
| 576.105 | 24.754 | 0.081 | 25.334 | 0.098 |
| 576.172 | 24.818 | 0.142 | 24.882 | 0.094 |
| 581.266 | 24.424 | 0.055 | 25.648 | 0.124 |
| 581.333 | 24.442 | 0.092 | 25.345 | 0.129 |
| 581.400 | 24.325 | 0.060 | ... | ... |
| 581.467 | ... | ... | 24.928 | 0.077 |
| 581.534 | 24.366 | 0.080 | 25.207 | 0.130 |
| 581.601 | 24.450 | 0.061 | 25.669 | 0.192 |

NOTE. — The complete version of this table is in the electronic edition of the Journal. The printed edition contains only a sample.

TABLE 5
V PHOTOMETRY OF THE VARIABLE STARS IN AND I

| HJD-2449000 | V01 | | V02 | |
|-------------|----------|------------|----------|------------|
| | <i>V</i> | σ_V | <i>V</i> | σ_V |
| 575.636 | 24.564 | 0.113 | 24.928 | 0.084 |
| 575.703 | 24.531 | 0.060 | 25.126 | 0.076 |
| 575.770 | 24.575 | 0.063 | 24.862 | 0.093 |
| 580.998 | 24.340 | 0.089 | 24.734 | 0.081 |
| 581.065 | 24.292 | 0.058 | 24.576 | 0.075 |
| 581.132 | 24.271 | 0.071 | 24.734 | 0.042 |
| 581.199 | 24.376 | 0.060 | 24.856 | 0.069 |

NOTE. — The complete version of this table is in the electronic edition of the Journal. The printed edition contains only a sample.

TABLE 6
B PHOTOMETRY OF THE VARIABLE STARS IN AND III

| HJD-2451000 | V01 | | V02 | |
|-------------|----------|------------|----------|------------|
| | <i>B</i> | σ_B | <i>B</i> | σ_B |
| 231.743 | ... | ... | 25.439 | 0.217 |
| 231.762 | 23.557 | 0.068 | 25.499 | 0.197 |
| 231.811 | 23.668 | 0.081 | 25.303 | 0.250 |
| 231.829 | 23.796 | 0.051 | 25.436 | 0.194 |
| 231.878 | 23.940 | 0.097 | 24.448 | 0.141 |
| 231.897 | 23.971 | 0.080 | 24.751 | 0.130 |
| 231.952 | 24.173 | 0.084 | 24.872 | 0.097 |
| 232.022 | 24.219 | 0.078 | 25.141 | 0.125 |
| 236.515 | 23.692 | 0.111 | 25.762 | 0.261 |
| 236.533 | 23.152 | 0.104 | ... | ... |
| 236.582 | 22.807 | 0.080 | 24.864 | 0.172 |
| 236.601 | 22.924 | 0.117 | 24.590 | 0.133 |
| 236.649 | 22.962 | 0.111 | 24.738 | 0.200 |
| 236.667 | 23.195 | 0.116 | 24.889 | 0.104 |
| 236.716 | 23.356 | 0.118 | 25.027 | 0.138 |
| 236.735 | 23.439 | 0.113 | 25.387 | 0.126 |

NOTE. — The complete version of this table is in the electronic edition of the Journal. The printed edition contains only a sample.

TABLE 7
V PHOTOMETRY OF THE VARIABLE STARS IN AND III

| HJD-2451000 | V01 | | V02 | |
|-------------|--------|------------|--------|------------|
| | V | σ_V | V | σ_V |
| 231.613 | 22.916 | 0.033 | 25.265 | 0.203 |
| 231.631 | 23.000 | 0.047 | 25.147 | 0.097 |
| 231.675 | 23.131 | 0.032 | 25.325 | 0.165 |
| 231.694 | 23.191 | 0.048 | 25.337 | 0.120 |
| 236.381 | 23.967 | 0.073 | 25.262 | 0.137 |
| 236.399 | ... | ... | 25.341 | 0.144 |
| 236.446 | 24.110 | 0.059 | 25.355 | 0.078 |
| 236.464 | 24.116 | 0.065 | 25.326 | 0.096 |

NOTE. — The complete version of this table is in the electronic edition of the Journal. The printed edition contains only a sample.

TABLE 8
ABSOLUTE MAGNITUDES OF THE SUPRA-HB STARS IN AND I AND AND III

| System | ID | Mode | M_V | M_B | Classification |
|---------|-----|------|-------|-------|----------------|
| And I | V01 | ... | -0.31 | -0.03 | P2C or AC? |
| And III | V01 | H | -1.03 | -0.88 | AC |
| | V06 | H | -1.38 | -1.03 | AC |
| | V07 | H | -0.55 | -0.15 | AC |
| | V08 | ... | -0.25 | 0.22 | P2C or AC? |
| | V09 | F | 0.03 | 0.39 | AC |

TABLE 9
FREQUENCY OF ANOMALOUS CEPHEIDS IN DWARF SPHEROIDAL GALAXIES

| Galaxy | $\langle [\text{Fe}/\text{H}] \rangle$ | M_V | PA (degrees) | $1-b/a$ | r_{exp} (arcsec) | Surveyed L (%) | N_{AC} | S | $\log S$ | References |
|---------|--|-------|-----------------|---------|------------------------------|---------------------|-----------------|------|-------------------------|------------|
| And I | -1.5 | -11.7 | 0 | 0.0 | 1.40 | 17 | 1 | 0.15 | $-0.82^{+0.31}_{-0.16}$ | 1,2,3 |
| And III | -1.9 | -10.2 | 136 | 0.6 | 0.75 | 25 | 5 | 2.1 | $0.32^{+0.16}_{-0.24}$ | 1,2,4 |

NOTE. — PA is the position angle measured from the North to the East. References: (1) Caldwell et al. (1992); (2) This paper; (3) Da Costa et al. (2000); (4) Da Costa et al. (2002). For the purposes of the discussion within the text we have assumed that And I - V01 and And III - V08 are anomalous Cepheids, but their true nature is still uncertain (see §4).